A chemical screen based on an interruption of zebrafish gastrulation identifies the HTR2C inhibitor Pizotifen as a suppressor of EMT-mediated metastasis

Joji Nakayama[1,2,3,4,§], Lora Tan[1], Boon Cher Goh[2], Shu Wang[1, 5], Hideki Makinoshima[3,6] and Zhiyuan Gong[1,§]

[1]Department of Biological Science, National University of Singapore, Singapore
[2]Cancer Science Institute of Singapore, National University of Singapore, Singapore
[3]Tsuruoka Metabolomics Laboratory, National Cancer Center, Tsuruoka, Japan
[4]Shonai Regional Industry Promotion Center, Tsuruoka, Japan.
[5]Institute of Bioengineering and Nanotechnology, Singapore
[6]Division of Translational Research, Exploratory Oncology Research and Clinical Trial Center, National Cancer Center, Kashiwa, Japan.

[§]Corresponding authors:
Joji Nakayama
email: Zmetastasis@gmail.com

Zhiyuan Gong
email: dbsgzy@nus.edu.sg

Keywords: Metastasis, gastrulation, EMT, Phenotyping screening, zebrafish

Total words excluding supplemental figure legends and references section: 5468

Number of figures: 5
Number of tables: 1
Number of supplemental figures: 3
Number of supplemental tables: 2

Abstract

Metastasis is responsible for approximately 90% of cancer-associated mortality but few models exist that allow for rapid and effective screening of anti-metastasis drugs. Current mouse models of metastasis are too expensive and time consuming to use for rapid and high-throughput screening. Therefore, we created a unique screening concept utilizing conserved mechanisms between zebrafish gastrulation and cancer metastasis for identification of potential anti-metastatic drugs. We hypothesized that small chemicals that interrupt zebrafish gastrulation might also suppress metastatic progression of cancer cells and developed a phenotype-based chemical screen to test the hypothesis. The screen used epiboly, the first morphogenetic movement in gastrulation, as a marker and enabled 100 chemicals to be tested in five hours. The screen tested 1280 FDA-approved drugs and identified Pizotifen, an antagonist for serotonin receptor 2C (HTR2C) as an epiboly-interrupting drug. Pharmacologic and genetic inhibition of HTR2C suppressed metastatic progression in a mouse model. Blocking HTR2C with Pizotifen restored epithelial properties to metastatic cells through inhibition of Wnt-signaling. In contrast, HTR2C induced epithelial to mesenchymal transition (EMT) through activation of Wnt-signaling and promoted metastatic dissemination of human cancer cells in a zebrafish xenotransplantation model. Taken together, our concept offers a novel platform for discovery of anti-metastasis drugs.

Introduction

Metastasis, a leading contributor to the morbidity of cancer patients, occurs through multiple steps: invasion, intravasation, extravasation, colonization, and metastatic tumor formation (1-3). The physical translocation of cancer cells is an initial step of metastasis and molecular mechanisms of it involve cell motility, the breakdown of local basement membrane, loss of cell polarity, acquisition of stem cell-like properties, and EMT (4-6). These cell-biological phenomena are also observed during vertebrate gastrulation in that evolutionarily conserved morphogenetic movements of epiboly, internalization, convergence, and extension progress (7). In zebrafish, the first morphogenetic movement, epiboly, is initiated at approximately 4 hours post fertilization (hpf) to move cells from the animal pole to eventually engulf the entire yolk cell by 10 hpf (8, 9). The embryonic cell movements are governed by the molecular mechanisms that are partially shared in metastatic cell dissemination.

At least fifty common genes were shown to be involved in both metastasis and gastrulation progression: Knockdown of these genes in Xenopus or zebrafish induced gastrulation defects; conversely, overexpression of these genes conferred metastatic potential on cancer cells and knockdown of these genes suppressed metastasis (Table S1). This evidence led us to hypothesize that small molecules that interrupt zebrafish gastrulation may suppress metastatic progression of human cancer cells.

Here we report a unique screening concept based on the hypothesis. Pizotifen, an antagonist for HTR2C, was identified from the screen as a “hit” that interrupted zebrafish gastrulation. A mouse model of metastasis confirmed pharmacological and genetic inhibition of HTR2C suppressed metastatic progression. Moreover, HTR2C induced EMT and promoted metastatic dissemination of non-metastatic cancer cells in a zebrafish xenotransplantation model. These results demonstrated that this concept could offer a novel high-throughput platform for discovery of anti-metastasis drugs and can be converted to a chemical genetic screening platform.

Results

Small molecules interrupting epiboly of zebrafish have a potential to suppress metastatic progression of human cancer cells.

Before performing a screening assay, we conducted preliminary experiments to test the hypothesis. First, we examined whether hindering the molecular function of reported genes, whose knockdown induced gastrulation defects in zebrafish, might suppress cell motility and invasion of cancer cells. We chose protein arginine methyltransferase 1 (PRMT1) and cytochrome P450 family 11 (CYP11A1), both of whose knockdown induced gastrulation defects in zebrafish but whose involvement in metastatic progression is unclear (10, 11). Elevated expression of PRMT1 and CYP11A1 were observed in highly metastatic human breast cancer cell lines and knockdown of these genes through RNA interference suppressed the motility and invasion of MDA-MB-231 cells without affecting their viability (Figure S1A-C).

Next, we conducted an inverse examination of whether chemicals which were reported to suppress metastatic dissemination of cancer cells could interrupt epiboly progression of zebrafish embryos. Niclosamide and Vinpocetine are reported to suppress metastatic progression (12, 13) (14, 15). Either Niclosamide or Vinpocetine-treated zebrafish embryos showed complete arrest at very early stages or severe delay in epiboly progression, respectively (Figure S1D).

These results suggest that epiboly could serve as a marker for this screening assay and epiboly-interrupting drugs that are identified through this screening could have the potential to suppress metastatic progression of human cancer cells.

132 FDA-approved drugs induced delayed in epiboly of zebrafish embryos

We screened 1,280 FDA, EMA or other agencies-approved drugs (Prestwick, Inc) in our zebrafish assay. The screening showed that 0.9% (12/1280) of the drugs, including Actimycin A and Tolcapone, induced severe or complete arrest of embryonic cell

103 movement when embryos were treated with 10μM. 5.2% (66/1280) of the drugs, such as
104 Dicumarol, Racecadotril, Pizotifen and S(-) Eticlopride hydrochloride, induced either
105 delayed epiboly or interrupted epiboly of the embryos. 93.3% (1194/1280) of drugs has
106 no effect on epiboly progression of the embryos. 0.6% (8/1280) of drugs induced a toxic
107 lethality. Epiboly progression was affected more severely when embryos were treated
108 with 50μM; 1.7% (22/1280) of the drugs induced severe or complete arrest of it. 8.6%
109 (110/1280) of the drugs induced either delayed epiboly or interrupt epiboly of the
110 embryos. 4.3% (55/1280) of drugs induced a toxic lethality (Figure 1A and 1B, Table S2).
111 Among the epiboly-interrupting drugs, several drugs have already been reported to inhibit
112 metastasis-related molecular mechanisms: Adrenosterone or Zardaverine, which target
113 HSD11β1 or PDE3 and 4, respectively, are reported to inhibit EMT (16, 17);
114 Racecadotril, which targets enkephalinase, is reported to confer metastatic potential on
115 colon cancer cell (18); and Disulfiram, which targets ALDH, is reported to confer stem-
116 like properties on metastatic cancer cells (19). This evidence suggests that epiboly-
117 interrupting drugs have the potential for suppressing metastasis of human cancer cells.
118
119 **Identified drugs suppressed cell motility and invasion of human cancer cells.**
120 It has been reported that zebrafish have orthologues to 86% of 1318 human drug targets
121 (20). However, it was not known whether the epiboly-interrupting drugs could suppress
122 metastatic dissemination of human cancer cells. To test this, we subjected the 78 epiboly-
123 interrupting drugs that showed a suppressor effect on epiboly progression at a 10μM
124 concentration to *in vitro* experiments using a human cancer cell line. The experiments
125 examined whether the drugs could suppress cell motility and invasion of MDA-MB-231
126 cells through a Boyden chamber. Before conducting the experiment, we investigated
127 whether these drugs might effect viability of MDA-MB-231 cells using an MTT assay.
128 Sixteen of the 78 drugs strongly effected cell viability at concentrations less than 1μM
129 and were not used in the cell motility experiments. The remaining 62 drugs were assayed

130 in Boyden chamber motility experiments. Twenty of the 62 drugs inhibited cell motility
131 and invasion of MDA-MB-231 cells without effecting cell viability. Among the 20 drugs,
132 Hexachlorophene and Nitazoxanide were removed since the primary targets of the drugs,
133 D-lactate dehydrogenase and pyruvate ferredoxin oxidoreductase are not expressed in
134 mammalian cells. With the exception of Ipriflavone, whose target is still unclear, the
135 known primary targets of the remaining 17 drugs are reported to be expressed by
136 mammalian cells (Figure 2A and Table 1).
137 We confirmed if highly metastatic human cancer cell lines expressed the genes
138 that code for these targets using Western blotting analyses. Among the genes, serotonin
139 receptor 2C (HTR2C), which is a primary target of Pizotifen, was highly expressed in
140 only metastatic cell lines (Figure 2B). Pizotifen suppressed cell motility and invasion of
141 several highly metastatic human cancer cell lines in a dose-dependent manner (Figure
142 2C). Similarly, Dopamine receptor D2 (DRD2), which is a primary target of S(-)
143 Eticlopride hydrochloride, was highly expressed in only metastatic cell lines, and the drug
144 suppressed cell motility and invasion of these cells in a dose-dependent manner (Figure
145 S2).
146 These results indicate that a number of the epiboly-interrupting drugs also have
147 suppressor effects on cell motility and invasion of highly metastatic human cancer cells.
148
149 **Pizotifen suppressed metastatic dissemination of human cancer cells in a zebrafish**
150 **xenotransplantation model.**
151 While a number of the epiboly-interrupting drugs suppressed cell motility and invasion of
152 human cell lines *in vitro,* it was still unclear whether the drugs could suppress metastatic
153 dissemination of cancer cells in vivo. Therefore, we examined whether the identified
154 drugs could suppress metastatic dissemination of these human cancer cells in a zebrafish
155 xenotransplantation model. Pizotifen was selected to test since HTR2C was overexpressed
156 only in highly metastatic cell lines supporting the hypothesis that it could be a novel target

157 for blocking metastatic dissemination of cancer cells (Figure 2B). Red fluorescent
158 protein-labelled MDA-MB-231 (231R) cells were injected into the duct of Cuvier of *Tg*
159 *(kdrl:eGFP)* zebrafish at 2 dpf and then maintained in the presence of either vehicle or
160 Pizotifen. Twenty-four hours post-injection, the numbers of fish showing metastatic
161 dissemination of 231R cells were measured via fluorescence microscopy. In this model,
162 the dissemination patterns were generally divided into three categories: (i) head
163 dissemination, in which disseminated 231R cells exist in the vessel of the head part; (ii)
164 trunk dissemination, in which the cells were observed in the vessel dilating from the trunk
165 to the tail; (iii) end-tail dissemination, in which the cells were observed in the vessel of
166 the end-tail part (16).

167 Three independent experiments revealed that the frequencies of fish in the drug-
168 treated group showing head, trunk, or end-tail dissemination, significantly decreased to
169 55.3±7.5%, 28.5±5.0% or 43.5±19.1% when compared with those in the vehicle-treated
170 group; 95.8±5.8%, 47.1±7.7% or 82.6±12.7%. Conversely, the frequency of the fish in the
171 drug-treated group not showing any dissemination, significantly increased to 45.4±0.5%
172 when compared with those in the vehicle-treated group; 2.0±2.9% (Figure 2D).

173 Similar effects were observed in another xenograft experiments using an RFP-
174 labelled human pancreatic cancer cell line, MIA-PaCa-2 (MP2R). In the drug treated
175 group, the frequencies of the fish showing head, trunk or end-tail dissemination,
176 significantly decreased to 15.3±6.7%, 6.2±1.3%, or 41.1±1.5%; conversely, the frequency
177 of the fish not showing any dissemination significantly increased to 46.3±8.9% when
178 compared with those in the vehicle-treated group; 74.5±11.1%, 18.9±14.9%, 77.0±9.0%,
179 or 17.2±0.7% (Figure S3).

180 To eliminate the possibility that the metastasis suppressing effects of Pizotifen
181 might result from off-target effects of the drug, we conducted validation experiments to
182 determine whether knockdown of HTR2C would show the same effects. Sub-clones of
183 231R cells that expressed shRNA targeting either LacZ or HTR2C were injected into the

184 fish at 2 dpf and the fish were maintained in the absence of drug. In the fish that were
185 inoculated with shHTR2C 231R cells, the frequencies of the fish showing head, trunk,
186 and end-tail dissemination, significantly decreased to 6.7±4.9%, 6.7±0.7%, or
187 20.0±16.5%; conversely, the frequency of the fish not showing any dissemination,
188 significantly increased to 80.0±4.4% when compared with those that were inoculated with
189 shLacZ 231R cells; 80.0±27.1%, 20.0±4.5%, 90.0± 7.7%, or 0% (Figure 2E).
190 These results indicate that pharmacological and genetic inhibition of HTR2C
191 suppressed metastatic dissemination of human cancer cells in vivo.
192
193 **Pizotifen suppressed metastasis progression of a mouse model of metastasis.**
194 We examined the metastasis-suppressor effect of Pizotifen in a mouse model of
195 metastasis (21). Luciferase-expressing 4T1 murine mammary carcinoma cells were
196 inoculated into the mammary fat pads (MFP) of female BALB/c mice. On day two
197 post inoculation, the mice were randomly assigned to two groups and one group
198 received once daily intraperitoneal injections of 10mg/kg Pizotifen while the other
199 group received a vehicle injection. Bioluminescence imaging and tumor measurement
200 revealed that the sizes of the primary tumors in Pizotifen-treated mice were equal to
201 those in the vehicle-treated mice at the time of resection on day 10 post inoculation.
202 Immunofluorescent staining also demonstrated that the percentage of Ki67 positive
203 cells in the resected primary tumors of Pizotifen-treated mice were the same as those
204 of vehicle-treated mice (Figure 3A-C), additionally, both groups showed less than 1%
205 cleaved caspase 3 positive cells (data not shown). Therefore, no anti-tumor effect of
206 Pizotifen was observed on the primary tumor. After 70 days from inoculation,
207 bioluminescence imaging detected light emitted in the lungs, livers and lymph nodes
208 of vehicle-treated mice but not those of Pizotifen-treated mice (Figure 3C). Vehicle-
209 treated mice formed 5 to 50 metastatic nodules per lung in all 10 mice analyzed;
210 conversely, Pizotifen-treated mice (n=10) formed 0 to 5 nodules per lung in all 10

211 mice analyzed (Figure 3D). Histological analyses confirmed that metastatic lesions in
212 the lungs were detected in all vehicle-treated mice; conversely, they were detected in
213 only 2 of 10 Pizotifen-treated mice and the rest of the mice showed metastatic colony
214 formations around the bronchiole of the lung. In addition, 4 of 10 vehicle-treated mice
215 exhibited metastasis in the liver and the rest showed metastatic colony formation
216 around the portal tract of the liver. In contrast, none of 10 Pizotifen-treated mice
217 showed liver metastases and only half of the 10 mice showed metastatic colony
218 formation around the portal tract (Figure 3E). These results indicate that Pizotifen can
219 suppress metastasis progression without affecting primary tumor growth.
220 To eliminate the possibility that the metastasis suppressing effects of Pizotifen
221 might result from off-target effects, we conducted validation experiments to determine
222 whether knockdown of HTR2C would show the same effects. The basic experimental
223 process followed the experimental design described above except that sub-clones of
224 4T1 cells that expressed shRNA targeting either LacZ or HTR2C were injected into
225 the MFP of female BALB/c mice and the mice were maintained without drug.
226 Histological analyses revealed that all of the mice (n=5) that were inoculated with 4T1
227 cells expressing shRNA targeting LacZ showed metastases in the lungs. The mean
228 number of metastatic lesions in a lung was 26.4±7.8. In contrast, only one of the mice
229 (n=5) were inoculated with 4T1 cells expressing shRNA targeting HTR2C showed
230 metastases in the lungs and the rest of the mice showed metastatic colony formation
231 around the bronchiole of the lung. The mean number of metastatic lesions in the lung
232 significantly decreased to 10% of those of mice that were inoculated with 4T1 cells
233 expressing shRNA targeting LacZ (Figure 3F-H).
234 Taken together, pharmacological and genetic inhibition of HTR2C showed an
235 anti-metastatic effect in the 4T1 model system.
236

237 **HTR2C promoted EMT-mediated metastatic dissemination of human cancer cells**

238 Although pharmacological and genetic inhibition of HTR2C inhibited metastasis
239 progression, a role for HTR2C on metastatic progression has not been reported.
240 Therefore, we examined whether HTR2C could confer metastatic properties on poorly
241 metastatic cells.

242 Firstly, we established a stable sub-clone of MCF7 human breast cancer cells
243 expressing either vector control or HTR2C. Vector control expressing MCF7 cells
244 maintained highly organized cell-cell adhesion and cell polarity; however, HTR2C-
245 expressing MCF7 cells led to loss of cell-cell contact and cell scattering. The cobblestone-
246 like appearance of these cells was replaced by a spindle-like, fibroblastic morphology.
247 Western blotting and immunofluorescence (IF) analyses revealed that HTR2C-expressing
248 MCF7 cells showed loss of E-cadherin and EpCAM, and elevated expressions of N-
249 cadherin, vimentin and an EMT-inducible transcriptional factor Zeb1. Similar effects
250 were validated through another experiment using an immortal keratinocyte cell line,
251 HaCaT cells, in that HTR2C-expressing HaCaT cells also showed loss of cell-cell contact
252 and cell scattering with loss of epithelial markers and gain of mesenchymal markers
253 (Figure 4A-C). Therefore, both the morphological and molecular changes in the HTR2C-
254 expressing MCF7 and HaCaT cells demonstrated that these cells had undergone an EMT.

255 Next, we examined whether HTR2C-driven EMT could promote metastatic
256 dissemination of human cancer cells. Boyden chamber assay revealed that HTR2C
257 expressing MCF7 cells showed an increased cell motility and invasion compared with
258 vector control-expressing MCF7 cells in vitro (Figure 4D). Moreover, we conducted in
259 vivo examination of whether HTR2C expression could promote metastatic dissemination
260 of human cancer cells in a zebrafish xenotransplantation model. Red fluorescence protein-
261 labelled MCF7 cells expressing either vector control or HTR2C were injected into the
262 duct of Cuvier of *Tg* (*kdrl:eGFP*) zebrafish at 2 dpf. Twenty-four hours post injection, the
263 frequencies of the fish showing metastatic dissemination of the inoculated cells were

264 measured using fluorescence microscopy. In the fish that were inoculated with HTR2C
265 expressing MCF7 cells, the frequencies of the fish showing head, trunk, and end-tail
266 dissemination significantly increased to 96.7±4.7%, 68.8±6.4%, or 89.5±3.4%;
267 conversely, the frequency of the fish not showing any dissemination decreased to 0%
268 when compared with those in the fish that were inoculated with vector control expressing
269 MCF7 cells; 33.1±18.5%, 0%, 56.9± 4.4%, or 43% (Figure 4E).
270 These results indicated that HTR2C promoted metastatic dissemination of cancer
271 cells though induction of EMT, and suggest that the screen can easily be converted to a
272 chemical genetic screening platform.
273
274 **Pizotifen induced mesenchymal to epithelial transition through inhibition of Wnt-**
275 **signaling.**
276 Finally, we elucidated the mechanism of action of how Pizotifen suppressed metastasis,
277 especially metastatic dissemination of cancer cells. Our results showed that HTR2C
278 induced EMT and that pharmacological and genetic inhibition of HTR2C suppressed
279 metastatic dissemination of MDA-MB-231 cells that had already transitioned to
280 mesenchymal-like traits via EMT. Therefore, we speculated that blocking HTR2C with
281 Pizotifen might inhibit the molecular mechanisms which follow EMT induction. We
282 firstly investigated the expressions of epithelial and mesenchymal markers in Pizotifen-
283 treated MDA-MB-231 cells since the activation of an EMT program needs to be transient
284 and reversible, and transition from a fully mesenchymal phenotype to a epithelial-
285 mesenchymal hybrid state or a fully epithelial phenotype is associated with malignant
286 phenotypes (22). IF and FACS analyses revealed 20% of Pizotifen-treated MDA-MB-231
287 cells restored E-cadherin expression. Also, western blotting analysis demonstrated that
288 4T1 primary tumors from Pizotifen-treated mice has elevated E-cadherin expression
289 compared with tumors from vehicle-treated mice (Figure 5A-C). However, mesenchymal
290 markers did not change between vehicle and Pizotifen-treated MDA-MB-231 cells (data

291 not shown). We further analyzed E-cadherin positive (E-cad$^+$) cells in Pizotifen-treated
292 MDA-MB-231 cells. The E-cad$^+$ cells showed elevated expressions of epithelial markers
293 KRT14 and KRT19; and decreased expression of mesenchymal makers vimentin, MMP1,
294 MMP3, and S100A4. Recent research reports that an EMT program needs to be transient
295 and reversible and that a mesenchymal phenotype in cancer cells is achieved by
296 constitutive ectopic expression of Zeb1. In accordance with the research, the E-cad$^+$ cells
297 and 4T1 primary tumors from Pizotifen-treated mice had decreased Zeb1 expression
298 compared with vehicle-treated cells and tumors from vehicle-treated mice (Figure 5D). In
299 contrast, HTR2C-expressing MCF7 and HuMEC cells expressed Zeb1 but not vehicle
300 control MCF7 and HuMEC cells (Figure 4C). These results indicate that HTR2C-
301 mediated signaling induced EMT through up-regulation of Zeb1 and blocking HTR2C
302 with Pizotifen induced mesenchymal to epithelial transition through downregulation of
303 Zeb1.

304 We further investigated the mechanism of action of how blocking HTR2C with
305 Pizotifen induced down-regulation of Zeb1. In embryogenesis, serotonin-mediated
306 signaling is required for Wnt-dependent specification of the superficial mesoderm during
307 gastrulation (23). In cancer cells, overexpression of HTR1D is associated with Wnt-
308 signaling which enables induction of EMT (24, 25). This evidence led to a hypothesis that
309 HTR2C-mediated signaling might turn on transcriptional activity of β-catenin and that
310 might induce up-regulation of EMT-TFs. IF analyses revealed β-catenin was accumulated
311 in the nucleus of HTR2C-expressing MCF7 cells but it was located in the cytoplasm of
312 vector control-expressing cells (Figure 5E). Nuclear accumulation of β-catenin in
313 HTR2C-expressing MCF7 cells was confirmed by western blot (Figure 5F). In contrast,
314 Pizotifen-treated MDA-MB-231 cells showed β-catenin located in the cytoplasm of the
315 cells. Vehicle-treated cells showed β-catenin accumulated in the nucleus of the cells.
316 (Figure 5G), and western blotting analysis confirmed that it was located in the cytoplasm
317 of Pizotifen-treated MDA-MB-231 cells (Figure 5H). Furthermore,

318 immunohistochemistry and western blotting analyses showed that β-catenin accumulated
319 in the nucleus, and phospho-GSKβ and Zeb1 expression were decreased in 4T1 primary
320 tumors from Pizotifen-treated mice compared with vehicle-treated mice (Figure 5C).
321 These results indicated that HTR2C would regulate transcriptional activity of β-catenin
322 and Pizotifen could inhibit it.
323 Taken together, we conclude that blocking HTR2C with Pizotifen restored
324 epithelial properties to metastatic cells (MDA-MB-231 and 4T1 cells) through a decrease
325 of transcriptional activity of β-catenin and that suppressed metastatic progression of the
326 cells.
327

328 **Figures and figure legends**

329 **Figure 1**

330

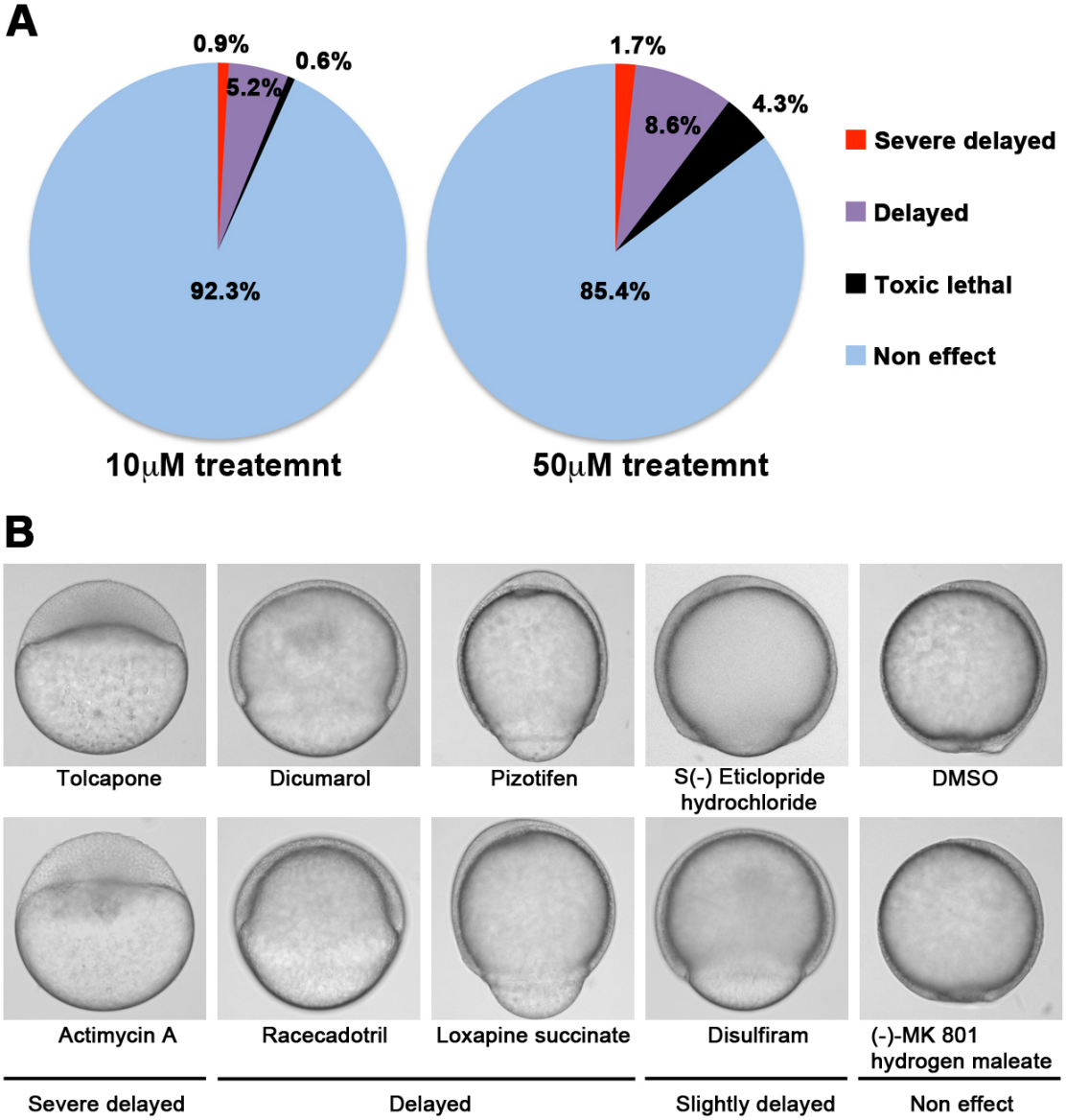

331

332

333 **Figure 1. A chemical screen for identification of epiboly-interrupting drugs.**

334 (A) Cumulative results of the chemical screen in which each drug was used at either

335 10μM (left) or 50μM (right) concentrations. 1,280 FDA, EMA or other agencies-

336 approved drugs were subjected to this screening. Positive "hit" drugs were those that

337 interrupted epiboly progression. (B) Representative samples of the embryos that were

338 treated with indicated drugs.

339 **Figure 2**

340

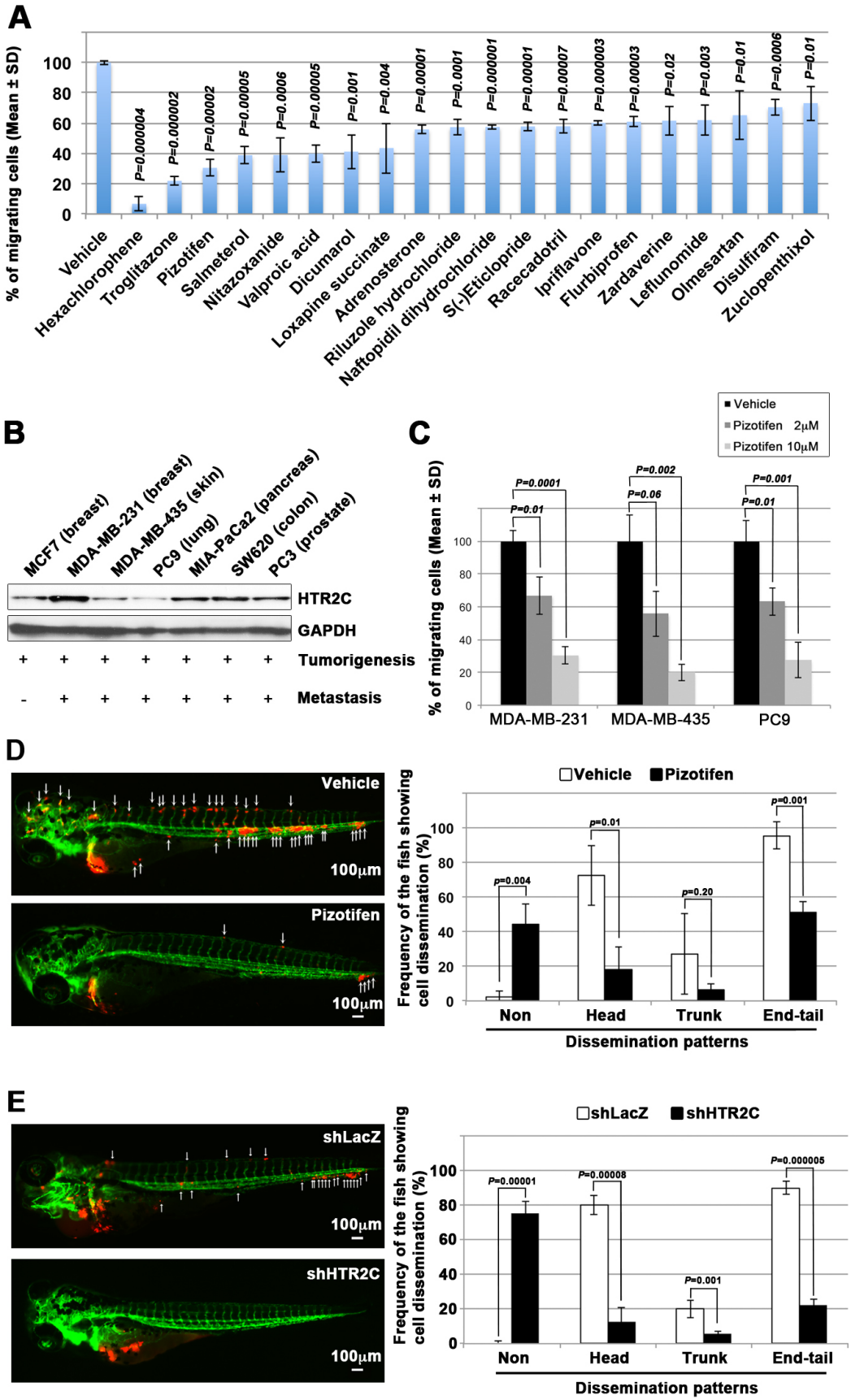

341

342 **Figure 2. Pizotifen, one of epiboly-interrupting drugs suppressed metastatic**

343 **dissemination of human cancer cells lines in vivo and vitro.**

344 (A) Effect of the epiboly-interrupting drugs on cell motility and invasion of MBA-MB-
345 231 cells. MBA-MB-231 cells were treated with vehicle or each of the epiboly-
346 interrupting drugs and then subjected to Boyden chamber assays. Fetal bovine serum
347 (1%v/v) was used as the chemoattractant in both assays. Each experiment was performed
348 at least twice. (B) Western blot analysis of HTR2C levels (top) in a non-metastatic human
349 cancer cell line, MCF7 (breast) and highly metastatic human cancer cell lines, MDA-MB-
350 231 (breast), MDA-MB-435 (melanoma), PC9 (lung), MIA-PaCa2 (pancreas), PC3
351 (prostate) and SW620 (colon); GAPDH loading control is shown (bottom). (C) Effect of
352 pizotifen on cell motility and invasion of MBA-MB-231, MDA-MB-435 and PC9 cells.
353 Either vehicle or pizotifen treated the cells were subjected to Boyden chamber assays.
354 Fetal bovine serum (1%v/v) was used as the chemoattractant in both assays. Each
355 experiment was performed at least twice. (D) and (E) Representative images of
356 dissemination of 231R, shLacZ 231R or shHTR2C 231R cells in zebrafish
357 xenotransplantation model. The fish larvae that were inoculated with 231R cells, were
358 treated with either vehicle (top left) or the drug (lower left) (D). The fish larvae that were
359 inoculated with either shLacZ 231R or shHTR2C 231R cells (lower left) (E). White
360 arrows head indicate disseminated 231R cells. The images were shown in 4x
361 magnification. Scale bar, 100μm. The mean frequencies of the fish showing head, trunk,
362 or end-tail dissemination were counted (graph on right). Each value is indicated as the
363 mean ± SEM of two independent experiments. Statistical analysis was determined by
364 Student's t test. See also Figure S2 and S3.
365

366 **Figure 3**

367

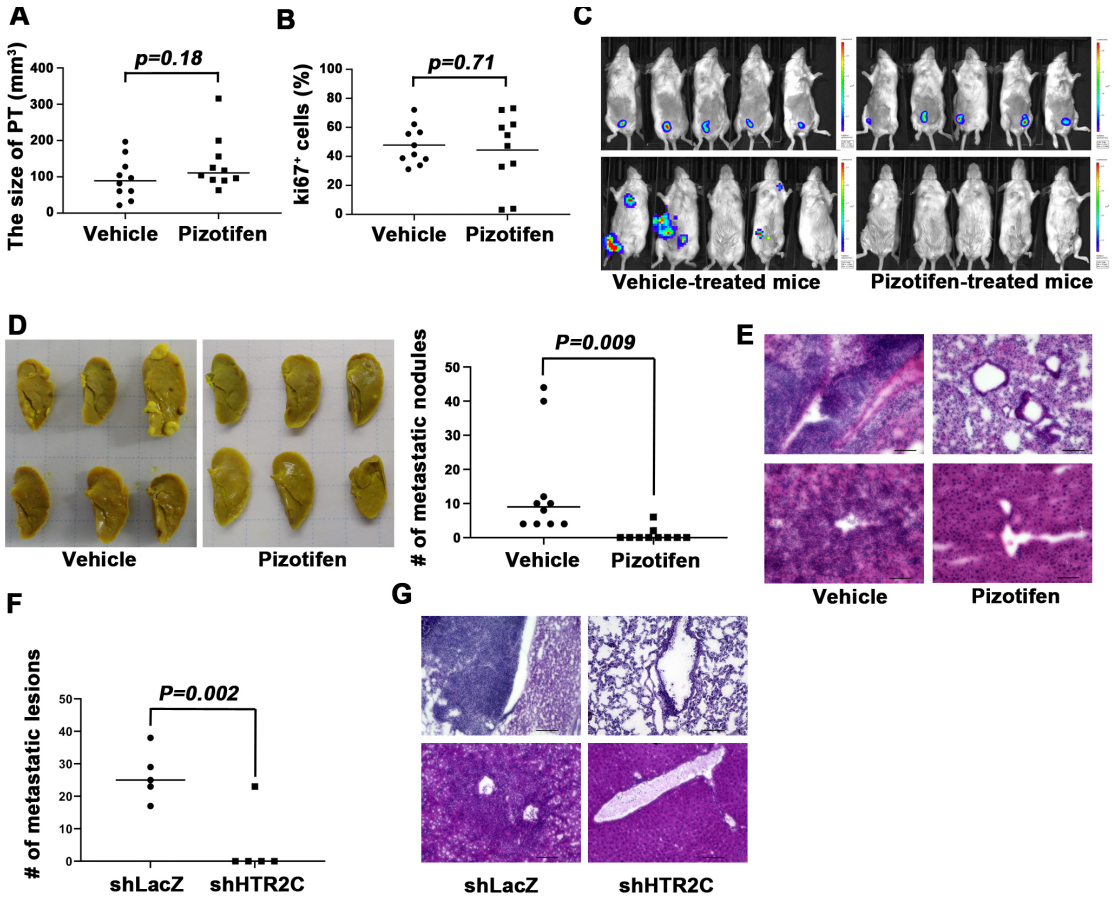

368

369

370 **Figure 3. Pizotifen suppressed metastatic progression in a mouse model of**

371 **metastasis.**

372 (A) Mean volumes (n=10 per group) of 4T1 primary tumors formed in the mammary fat

373 pad of either vehicle or Pizotifen-treated mice at day 10 post injection. (B) Ki67

374 expression level in 4T1 primary tumors formed in the mammary fat pad of either vehicle

375 or Pizotifen-treated mice at day 10 post injection. The mean expression levels of Ki67

376 (n=10 mice per group) were determined and were calculated as the mean ration of Ki67

377 positive cells to DAPI area. (C) Representative images of primary tumors on day 10 post

378 injection (top panels) and metastatic burden on day 70 post injection (bottom panels)

379 taken using an IVIS Imaging System. (D) Representative images of the lungs from either

380 vehicle (top) or Pizotifen-treated mice (bottom) at 70 days past tumor inoculation.

381 Number of metastatic nodules in the lung of either vehicle or Pizotifen-treated mice
382 (right). (E) Representative H&E staining of the lung (top) and liver (bottom) from either
383 vehicle or Pizotifen-treated mice. (F) The mean number of metastatic lesions in step
384 sections of the lungs from the mice that were inoculated with 4T1-12B cells expressing
385 shRNA targeting for either LacZ or HTR2C. (G) Representative H&E staining of the lung
386 and liver from the mice that were inoculated with 4T1-12B cells expressing shRNA
387 targeting for either LacZ or HTR2C. Each value is indicated as the mean ± SEM.
388 Statistical analysis was determined by Student's *t* test.
389

390 **Figure 4**

391

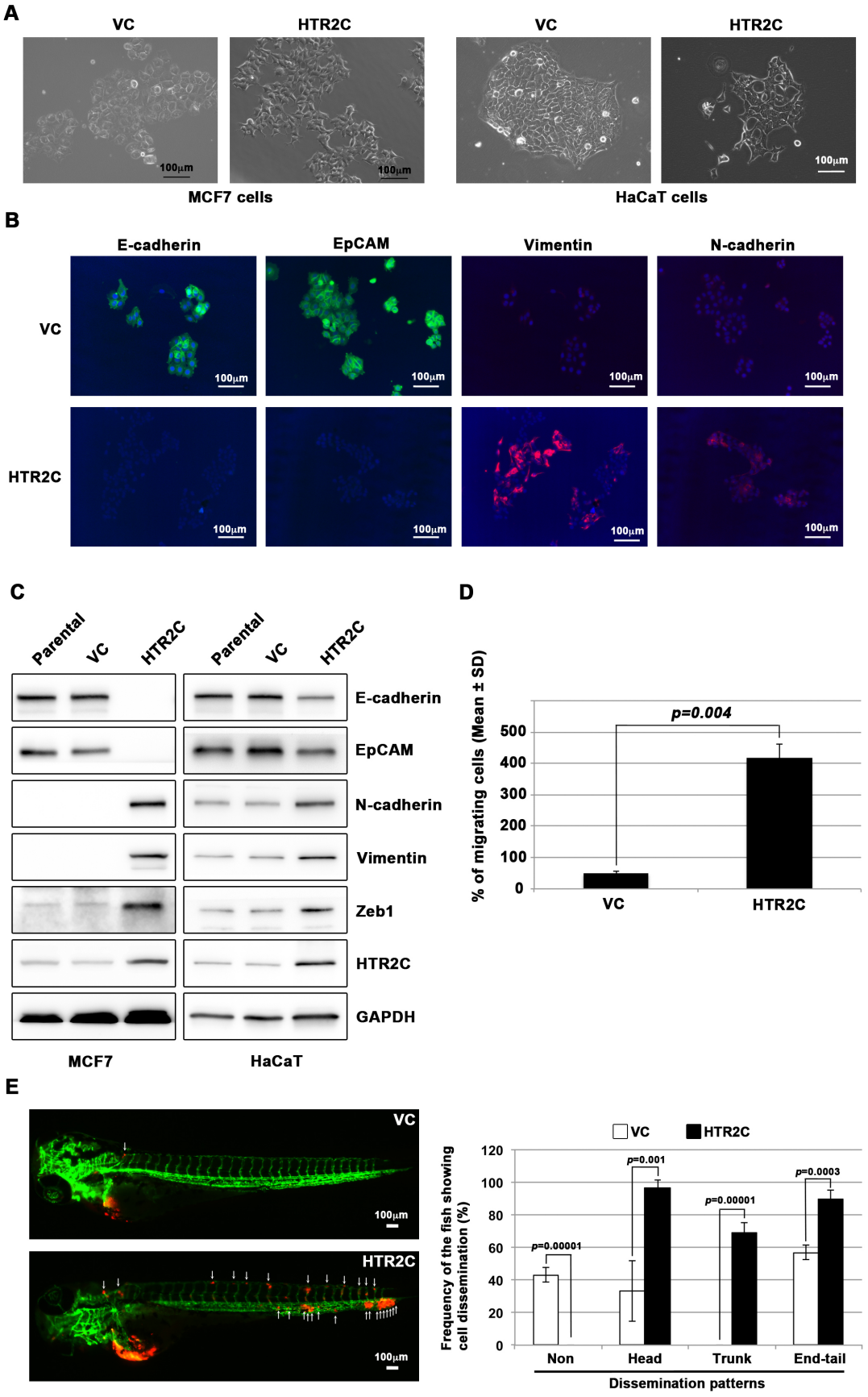

392

393 **Figure 4. HTR2C induced EMT-mediated metastatic dissemination of human cancer**
394 **cells.**
395 (A) The morphologies of the MCF7 and HaCaT cells expressing either the control vector
396 or HTR2C were revealed by phase contrast microscopy. (B) Immunofluorescence staining
397 of E-cadherin, EpCAM, Vimentin, and N-cadherin expressions in the MCF7 cells from
398 Figure 4A. (C) Expression of E-cadherin, EpCAM, Vimentin, N-cadherin, and HTR2C
399 was examined by western-blotting in the MCF7 and HaCaT cells; GAPDH loading
400 control is shown (bottom). (D) Effect of HTR2C on cell motility and invasion of MCF7
401 cells. MCF7 cells were subjected to Boyden chamber assays. Fetal bovine serum (1%v/v)
402 was used as the chemoattractant in both assays. Each experiment was performed at least
403 twice. (E) Representative images of dissemination patterns of MCF7 cells expressing
404 either the control vector (top left) or HTR2C (lower left) in a zebrafish
405 xenotransplantation model. White arrows head indicate disseminated MCF7 cells. The
406 mean frequencies of the fish showing head, trunk, or end-tail dissemination tabulated
407 (right). Each value is indicated as the mean ± SEM of two independent experiments.
408 Statistical analysis was determined by Student's *t* test.
409

410 **Figure 5**

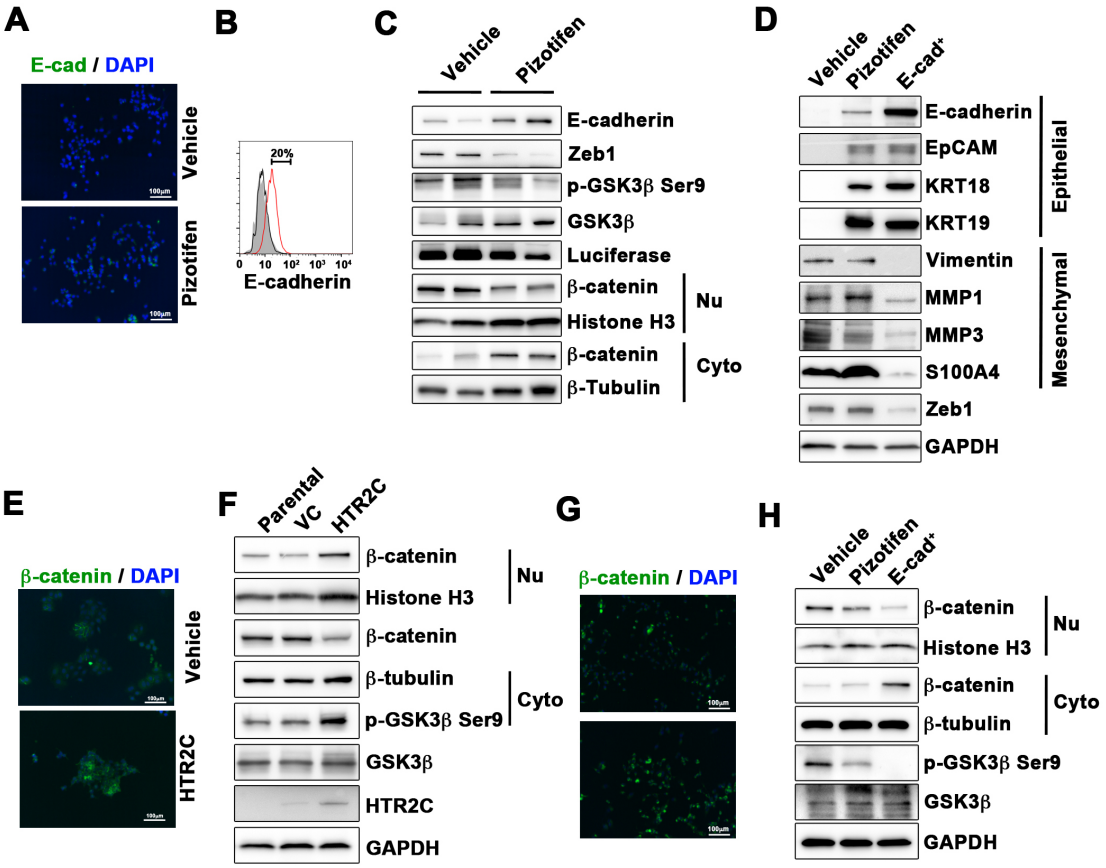

411

412 **Figure 5. Pizotifen restored mesenchymal-like traits of MDA-MB-231 cells into**

413 **epithelial traits through blocking nuclear accumulation of β-catenin.**

414 (A) IF staining of E-cadherin in either vehicle or Pizotifen-treated MDA-MB-231 cells.

415 (B) Surface expression of E-cadherin in either vehicle (black) or Pizotifen (red)-treated

416 MDA-MB-231 cells by FACS analysis. Non-stained controls are shown in gray. (C)

417 Protein expressions levels of E-cadherin, Zeb1, and β-catenin in the cytoplasm and

418 nucleus of 4T1 primary tumors from either vehicle or Pizotifen-treated mice are shown;

419 Luciferase, Histone H3, and β-tubulin are used as loading control for whole cell, nuclear

420 or cytoplasmic lysate, respectively. (D) Protein expression levels of epithelial and

421 mesenchymal markers and Zeb1 in either vehicle or Pizotifen-treated MDA-MB-231 cells

422 or E-cadherin positive (E-cad^{+}) cells in Pizotifen-treated MDA-MB-231 cells are shown.

423 (E) Immunofluorescence staining of β-catenin in the MCF7 cells expressing either vector

424 control or HTR2C. (F) Expressions of β-catenin in the cytoplasm and nucleus of MCF7

425 cells. (G) IF staining of β-catenin in either vehicle or Pizotifen-treated MDA-MB-231

426 cells. (H) Expressions of β-catenin in the cytoplasm and nucleus of MDA-MB-231 cells

427 and the E-cad^{+} cells.

428

429 **Table 1. Primary targets of the identified drugs**

430

The identified drugs	Primary targets of the identified drugs
Hexachlorophene	D-lactate dehydrogenase (D-LDH), not expressed in mammalian cells
Troglitazone	Agonist for Peroxisome proliferator-activated receptor α and γ (PPARα and γ)
Pizotifen malate	5-hydroxytryptamine receptor 2C (HTR2C)
Salmeterol	Adrenergic receptor beta 2 (ADRB2)
Nitazoxanide	Pyruvate ferredoxin oxidoreductase (PFOR), not expressed in mammalian cells
Valproic acid	Histone deacetylases (HDACs)
Dicumarol	NAD(P)H dehydrogenase quinone 1 (NQO1)
Loxapine succinate	Dopamine receptor D2 and D4 (DRD2 and DRD4)
Adrenosterone	Hydroxysteroid (11-beta) dehydrogenase 1 (HSD11β1)
Riluzole hydrochloride	Glutamate R and Voltage-dependent Na+ channel
Naftopidil dihydrochloride	5-hydroxytryptamine receptor 1A (HTR1A) and α1-adrenergic receptor (AR)
S(-)Eticlopride hydrochloride	Dopamine receptor D2 (DRD2)
Racecadotril	Membrane metallo-endopeptidase (MME)
Ipriflavone	Unknow
Flurbiprofen	Cyclooxygenase 1 and 2 (Cox1 and 2)
Zardaverine	Phosphodiesterase III/IV (PDE3/4)
Leflunomide	Dihydroorotate dehydrogenase (DHODH)
Olmesartan	Angiotensin II receptor alpha
Disulfiram	Aldehyde dehydrogenase (ALDH) Dopamine β-hydroxylase (DBH)
Zuclopenthixol dihydrochloride	Dopamine receptors D1 and D2 (DRD1 and 2)

431

432

433

434

435

436 **Discussion**

437 Reducing or eliminating mortality associated with metastatic disease is a key goal of
438 medical oncology, but few models exist that allow for rapid, effective screening of novel
439 compounds that target the metastatic dissemination of cancer cells. Based on accumulated
440 evidence that at least fifty genes play an essential role in governing both metastasis and
441 gastrulation progression (Table 1S), we hypothesized that small molecule inhibitors that
442 interrupt gastrulation of zebrafish embryos might suppress metastatic progression of
443 human cancer cells. We created a unique screening concept utilizing gastrulation of
444 zebrafish embryos to test the hypothesis. Our results clearly confirmed our hypothesis:
445 25.6% (20/76 drugs) of epiboly-interrupting drugs could also suppress cell motility and
446 invasion of highly metastatic human cell lines in vitro. In particular, Pizotifen which is an
447 antagonist for serotonin receptor 2C and one of the epiboly-interrupting drugs, could
448 suppress metastasis in a mouse model (Figure 3A-E). Thus, this screen could offer a novel
449 platform for discovery of anti-metastasis drugs.

450 There are at least two advantages to the screen described herein. One is that the
451 screen can easily be converted to a chemical genetic screening platform. Indeed, we have
452 provided the first evidence that HTR2C, which is a primary target of Pizotifen, induced
453 EMT and promoted metastatic dissemination of cancer cells (Figure 4A-E). In this
454 research, 1,280 FDA approval drugs were screened, this is less than a few percent of all of
455 druggable targets (approximately 100 targets) in the human proteome in the body. If
456 chemical genetic screening using specific inhibitor libraries were conducted, more genes
457 that contribute to metastasis and gastrulation could be identified. The second advantage is
458 that the screen enables one researcher to test 100 drugs in 5 hours with using optical
459 microscopy, drugs, and zebrafish embryos. That indicates this screen is not only highly
460 efficient, low-cost, and low-labor but also enables researchers who do not have high
461 throughput screening instruments to conduct drug screening for anti-metastasis drugs.
462

463 **Acknowledgments**

464 We sincerely appreciate Dr. Joshua Collins (NIH/NIDCR) and Dr. Diane Palmieri
465 (NIH/NCI) for helping this research. We thank Dr. Herrick (Albany medical collage) for
466 providing pCMV-h5TH2C-VSV with us. This study was funded by grants from National
467 Medical Research Council of Singapore (R-154000547511) and Ministry of Education of
468 Singapore (R-154000A23112) to Z.G.

469

470 **Author Contributions**

471 Design research; J.N. Conducting experiments; J.N. and L.T. Analyzing data: J.N.
472 Writing the paper; J.N. and Z.G. Funding Acquisition; Z.G, S.W. B.C.G., H.M. and
473 Supervision; Z.G.

474

475 **Declaration of Interests**

476 J.N., L.T., B.C.G., S.W., H.M. and G.Z. declare no conflict of interest.

477

478 **Materials and Methods**

479 **Zebrafish embryo screening**

480 Each drug was added to a well of a 24-well plate containing approximately 20 zebrafish
481 embryos per well in either 10 μM or 50 μM final concentration when the embryos reached
482 the sphere stage. Chemical treatment was initiated at 4 hours post-fertilization (hpf) and
483 approximately 20 embryos were treated with two different concentrations for each
484 compound tested. The treatment was ended at 9 hpf when vehicle (DMSO) treated
485 embryos as control reach 80-90% completion of the epiboly stage. The compounds which
486 induced delay (<50% epiboly) in epiboly were selected as hit compounds for in vitro
487 testing using highly metastatic human cancer cell lines. The study protocol was approved
488 by the Institutional Animal Care and Use Committee of the National University of
489 Singapore (protocol number: R16-1068).

490

491 **Reagents**

492 FDA, EMA and other agencies approved chemical libraries was purchased from
493 Prestwick Chemical (Illkirch, France). Pizotifen and S(-) Eticlopride hydrochloride were
494 purchased from Sigma-Aldrich (St. Louis, MO).

495

496 **Cell culture and cell viability assay**

497 MCF7, MDA-MB-231, MDA-MB-435, MIA-PaCa2, PC3, SW620, PC9 and HaCaT cells
498 were obtained from American Type Culture Collection (ATCC, Manassas, VA).
499 HCCLM3 cells were provided by Dr. Tang, Zhong Shan Hospital of Fudan University
500 (Shanghai, China). Luciferase-expressing 4T1 (4T1-12B) cells were provided from Dr.
501 Gary Sahagian (Tufts University, Boston, MA). All culture methods followed the
502 supplier's instruction. Cell viability assay was performed as previously described (16).

503

504 **Plasmid**

505 A DNA fragment coding for HTR2C was amplified by PCR with primers containing
506 restriction enzyme recognition sequences. The HTR2C coding fragment was amplified
507 from hsp70l:mCherry-T2A-CreERT2 plasmid (17).

508

509 **Immunoblotting**

510 Western blotting was performed as described previously (16). Anti-PRMT1, anti-
511 CYP11A1, anti-E-cadherin, anti-EpCAM, anti-Vimentin, anti-N-cadherin, anti-Zeb1,
512 anti-Histone H_3, anti-α-tubulin and anti-GAPDH antibodies were purchased from Cell
513 signaling Technology. Anti-HTR2C and anti-DRD2 antibodies were purchased form
514 Abcam. Anti-phospho-GSK3β (Ser9), anti-GSK3β, Anti-KRT18, anti-KRT19, anti-
515 MMP1, anti-MMP2, anti-S100A4, anti-Luciferase, and anti-β-catenin antibodies were
516 purchased from Santa Cruz.

517

518 **Flow cytometry**

519 Cells were stained with FITC-conjugated E-cadherin antibody (Biolegend, San Diego,
520 CA). Flow cytometry was performed as described (26) and analyzed with FlowJo
521 software (TreeStar, Ashland, OR).

522

523 **shRNA mediated gene knockdown**

524 The short hairpin RNA (shRNA)-expressing lentivirus vectors were
525 constructed using pLVX-shRNA1 vector (Clontech). PRMT1-shRNA_#3–targeting
526 sequence is GTGTTCCAGTATCTCTGATTA; PRMT1-shRNA_#4–targeting sequence
527 is TTGACTCCTACGCACACTTTG. CYP11A1-shRNA_#4–targeting sequence is
528 GCGATTCATTGATGCCATCTA; CYP11A1-shRNA_#4–targeting sequence is
529 GAAATCCAACACCTCAGCGAT. Human HTR2C-shRNA–targeting sequence is
530 TCATGCACCTCTGCGCTATAT. Mouse HTR2C-shRNA–targeting sequence is . LacZ-
531 shRNA– targeting sequence is CTACACAAATCAGCGATT.

532

533 **Immunofluorescence**

534 Immunofluorescence microscopy assay was performed by previously described (ref).
535 Goat anti-mouse and goat anti-rabbit immunoglobulin G (IgG) antibodies conjugated to
536 Alexa Fluor 488 (Life Technologies) and diluted at 1:100 were used. Nuclei were
537 visualized by the addition of 2μg/ml of 4', 6-diamidino-2-phenylindole (DAPI) and
538 photographed at 100x magnification by a fluorescent microscope (Zeiss, Germany).

539

540 **Boyden chamber cell motility and invasion assay**

541 These assays were performed by previously described (16). In Boyden chamber assay,
542 either $3x10^5$ MDA-MB-231, $1x10^6$ MDA-MB-435, or $5x10^5$ PC9 cells were applied to
543 each well in the upper chamber.

544

545 **Zebrafish xenotransplantation model**

546 *Tg(kdrl:eGFP)* zebrafish was provided by Dr. Stainier (Max Planck Institute for Heart and
547 Lung Research). Embryos that were derived from the line were maintained in E3 medium
548 containing 200μM 1-phenyl-2-thiourea (PTU). Approximately 100-400 Red fluorescence
549 protein (RFP)-labelled MBA-MB-231 or MIA-Paca2 cells were injected into the duct of
550 Cuvier of the zebrafish at 2dpf.

551

552 **Spontaneous metastasis mouse model**

553 4T1-12B cells ($2x10^4$) were injected into the #4 mammary fat pad while the mice were
554 anesthetized. To monitor tumor growth and metastases, mice were imaged biweekly by
555 IVIS Imaging System (ParkinElmer). The primary tumor was resected 10 days after
556 inoculation. The study protocol (protocol number: BRC IACUC #110612) was approved
557 by A*STAR (Agency for Science, Technology and Research, Singapore).

558

559 **Histological Analysis**

560 All OCT embedded primary tumors, lungs, and livers of mice from the spontaneous
561 metastasis 4T1 model were sectioned on a cryostat. Eight micron sections were taken at
562 five hundred micron intervals through the entirety of the livers and lungs. Sections were
563 subsequently stained with hematoxylin and eosin. Metastatic lesions were counted under a
564 microscope in each section for both lungs and livers.

565

566 **Statistics**

567 Data were analyzed by Student's t test; $p < 0.05$ was considered significant.

568

569 **References**

570 1. Chambers AF, Groom AC, & MacDonald IC (2002) Dissemination and
571 growth of cancer cells in metastatic sites. *Nature reviews. Cancer* 2(8):563-
572 572.
573 2. Steeg PS (2003) Metastasis suppressors alter the signal transduction of
574 cancer cells. *Nature reviews. Cancer* 3(1):55-63.
575 3. Fidler IJ (2003) The pathogenesis of cancer metastasis: the 'seed and soil'
576 hypothesis revisited. *Nature reviews. Cancer* 3(6):453-458.
577 4. Cavallaro U & Christofori G (2004) Cell adhesion and signalling by
578 cadherins and Ig-CAMs in cancer. *Nature reviews. Cancer* 4(2):118-132.
579 5. Ellenbroek SI, Iden S, & Collard JG (2012) Cell polarity proteins and
580 cancer. *Semin Cancer Biol* 22(3):208-215.
581 6. Tsai JH & Yang J (2013) Epithelial-mesenchymal plasticity in carcinoma
582 metastasis. *Genes & development* 27(20):2192-2206.
583 7. Solnica-Krezel L (2005) Conserved patterns of cell movements during
584 vertebrate gastrulation. *Curr Biol* 15(6):R213-228.
585 8. Latimer A & Jessen JR (2010) Extracellular matrix assembly and
586 organization during zebrafish gastrulation. *Matrix Biol* 29(2):89-96.
587 9. Solnica-Krezel L (2006) Gastrulation in zebrafish -- all just about
588 adhesion? *Curr Opin Genet Dev* 16(4):433-441.
589 10. Tsai YJ, *et al.* (2011) The predominant protein arginine methyltransferase
590 PRMT1 is critical for zebrafish convergence and extension during
591 gastrulation. *FEBS J* 278(6):905-917.
592 11. Hsu HJ, Liang MR, Chen CT, & Chung BC (2006) Pregnenolone stabilizes
593 microtubules and promotes zebrafish embryonic cell movement. *Nature*
594 439(7075):480-483.
595 12. Weinbach EC & Garbus J (1969) Mechanism of Action of Reagents that
596 uncouple Oxidative Phosphorylation. *Nature* 221:1016.
597 13. Sack U, *et al.* (2011) Novel effect of antihelminthic Niclosamide on
598 S100A4-mediated metastatic progression in colon cancer. *Journal of the*
599 *National Cancer Institute* 103(13):1018-1036.
600 14. Huang EW, *et al.* (2012) Vinpocetine inhibits breast cancer cells growth in
601 vitro and in vivo. *Apoptosis : an international journal on programmed cell*
602 *death* 17(10):1120-1130.
603 15. Szilágyi G, *et al.* (2005) Effects of vinpocetine on the redistribution of
604 cerebral blood flow and glucose metabolism in chronic ischemic stroke
605 patients: a PET study. *Journal of the Neurological Sciences* 229-230:275-
606 284.
607 16. Nakayama J, Lu J, Makinoshima H, & Gong Z (2020) A Novel Zebrafish
608 Model of Metastasis Identifies the HSD11β1 Inhibitor Adrenosterone as a
609 Suppressor of Epithelial-Mesenchymal Transition and Metastatic
610 Dissemination. *Mol Cancer Res* 18(3):477-487.
611 17. Kolosionek E, *et al.* (2009) Expression and activity of phosphodiesterase
612 isoforms during epithelial mesenchymal transition: the role of
613 phosphodiesterase 4. *Mol Biol Cell* 20(22):4751-4765.
614 18. Sasaki T, *et al.* (2014) Serum CD10 is associated with liver metastasis in
615 colorectal cancer. *J Surg Res.* 192(2):390-394.
616 19. Liu P, *et al.* (2013) Disulfiram targets cancer stem-like cells and reverses
617 resistance and cross-resistance in acquired paclitaxel-resistant triple-
618 negative breast cancer cells. *British journal of cancer* 109(7):1876-1885.
619 20. Gunnarsson L, Jauhiainen A, Kristiansson E, Nerman O, & Larsson DGJ
620 (2008) Evolutionary conservation of human drug targets in organisms

621 used for environmental risk assessments. *Environmental Science &*
622 *Technology* 42(15):5807-5813.
623 21. Tao K, Fang M, Alroy J, & Sahagian GG (2008) Imagable 4T1 model for the
624 study of late stage breast cancer. *BMC cancer* 8:228.
625 22. Kröger C, Afeyan, A.; Mraz, J.; Eaton, EN.; Reinhardt, F.; Khodor, YL.; Thiru,
626 P.; Bierie B.; Ye, X.; Burge, CB.; Weinberg RA (2019) Acquisition of a
627 hybrid E/M state is essential for tumorigenicity of basal breast cancer
628 cells. *Proceedings of the National Academy of Sciences of the United States*
629 *of America* 116(15):7353-7362.
630 23. Beyer TD, M.; Thumberger, T.; Vick, P.; Tisler, M.; Schneider, I.; Bogusch, S.;
631 Andre, P.; Ulmer, B.; Walentek, P.; Niesler, B.; Blum, M.; Schweickert, A.
632 (2012) Serotonin signaling is required for Wnt-dependent GRP
633 specification and leftward flow in Xenopus. *Curr Biol* 22(1):33-39.
634 24. Sui HX, H.; Ji, Q.; Liu, X.; Zhou, L.; Song, H.; Zhou, X.; Xu, Y.; Chen, Z.; Cai, J.;
635 Ji, G.; Li, Q. (2015) 5-hydroxytryptamine receptor (5-HT1DR) promotes
636 colorectal cancer metastasis by regulating Axin1/β-catenin/MMP-7
637 signaling pathway. *Oncotarget* 6(28):25975-25987.
638 25. Zhan TR, N.; Boutros, M. (2017) Wnt signaling in cancer. *Oncogene*
639 36(11):1461–1473.
640 26. Nakayama J*, et al.* (2009) BLNK suppresses pre-B-cell leukemogenesis
641 through inhibition of JAK3. *Blood* 113(7):1483-1492.
642

643

644 **Supplemental Information**

645

646 **Figure S1.**

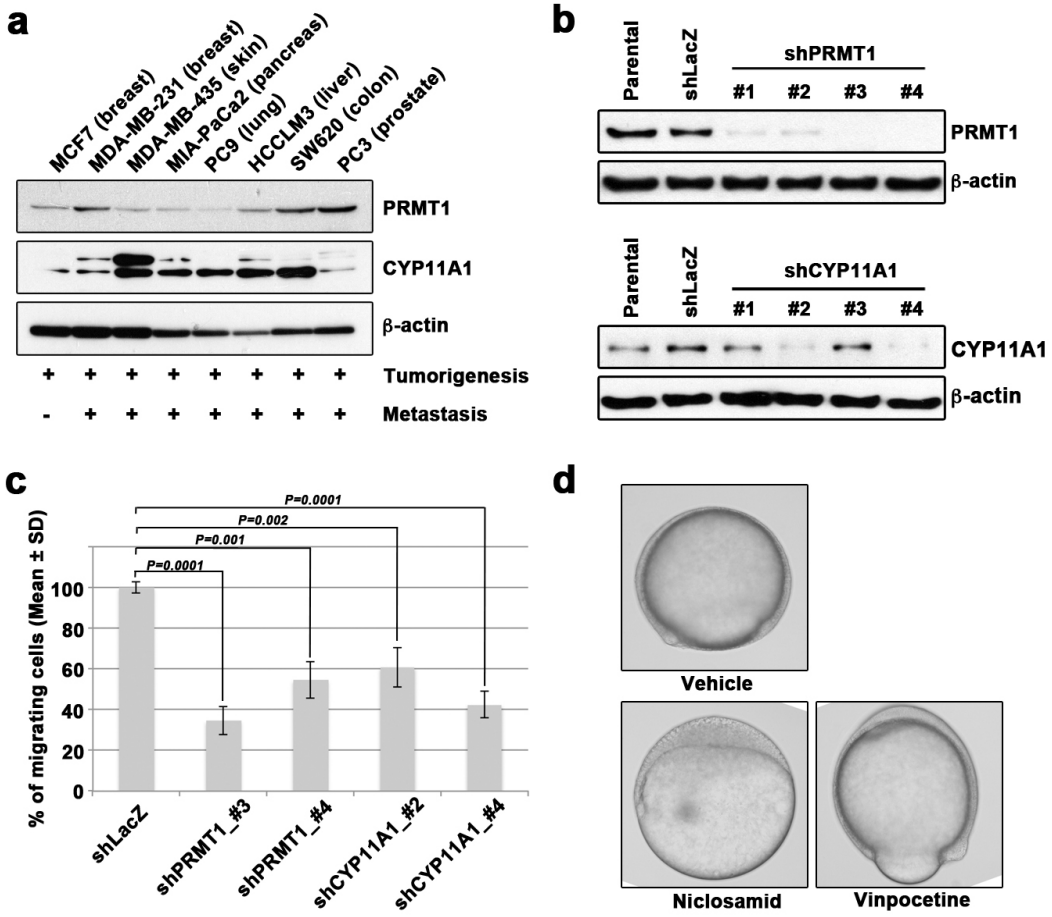

647

648

649 **Figure S1. Molecular mechanisms of epiboly in zebrafish overlap with those in**

650 **cancer metastasis.**

651 (A) Western blot analysis of PRMT1 (upper) and CYP11A1 (middle) protein levels in

652 non-metastatic human cancer cell line (MCF7) and highly metastatic human cancer

653 cell lines (MDA-MB-231, MDA-MB-435, MIA-PaCa2, PC9, HCCLM3, PC3 and

654 SW620); β-actin loading control is shown (bottom). (B) Knockdown of PRMT1 or

655 CYP11A1 in MDA-MB-231 cells. MBA-MB-231 cells were transfected with a

656 control shRNA targeting LacZ, and one of four independent shRNAs targeting

657 PRMT1 (clone #1 to #4) or one of two independent shRNAs targeting CYP11A1

658 (clone #1 to #4). Reduced PRMT1 and CYP11A1 expression, determined by western

659 blot, in sub-cell lines of MDA-MB-231 cells expressing PRMT1 shRNA (clone #3

660 and #4 or CYP11A1 (clone #2 and #4), compared with controls (parental cell line

661 MDA-MB-231 and control shRNA cells); β-actin levels shown as a loading control.
662 (C) Effect of shRNAs targeting either PRMT1 or CYP11A1 on cell motility and
663 invasion of MBA-MB-231 cells. Parental MDA-MB-231 cells and four sub-cell lines
664 of MDA-MB-231 cells that were transfected with either shRNA targeting either LacZ,
665 two independent shRNAs targeting PRMT1 (clone #3 and #4) or two independent
666 shRNAs targeting CYP11A1 (clone #2 and #4), were subjected to Boyden chamber
667 assays. (D) Zebrafish embryos treated with either vehicle (DMSO), 10μM
668 Niclosamide, or 50μM vinpocetine. Approximately 20 embryos were treated with
669 either DMSO as a vehicle control, niclosamide, or vinpocetine. The treatment was
670 started at 4 hpf when all of embryos reached sphere stage and ended at 9 hpf when
671 control embryos reached 80-90% epiboly stage. Each experiment was performed at
672 least twice. Statistical analysis was determined by Student's *t* test.
673

674 **Figure S2.**

675

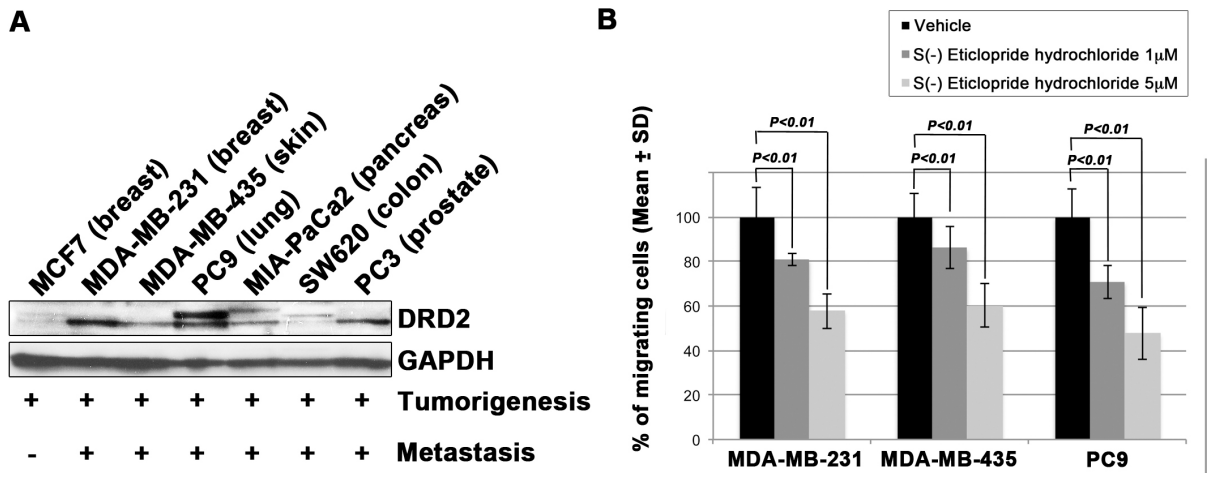

676

677

678 **Figure S2. S (-) Eticlopride hydrochloride suppressed cell motility and invasion of**

679 **human cancer cells.**

680 Related to Figure 2.

681 (A) Western blot analysis of DRD2 levels in non-metastatic human cancer cell line,

682 MCF7 (breast) and highly metastatic human cancer cell lines, MDA-MB-231 (breast),

683 MDA-MB-435 (melanoma), MIA-PaCa2 (pancreas), PC3 (prostate) and SW620 (colon);

684 GAPDH loading control is shown (bottom). (B) Effect of S (-) Eticlopride hydrochloride

685 on cell motility and invasion of MBA-MB-231, MDA-MB-435, and PC9 cells. Either

686 vehicle or pizotifen treated cells were subjected to Boyden chamber assays. Fetal bovine

687 serum (1%v/v) was used as the chemoattractant in both assays. Each experiment was

688 performed at least twice. Statistical analysis was determined by Student's *t* test.

689

690 **Figure S3.**

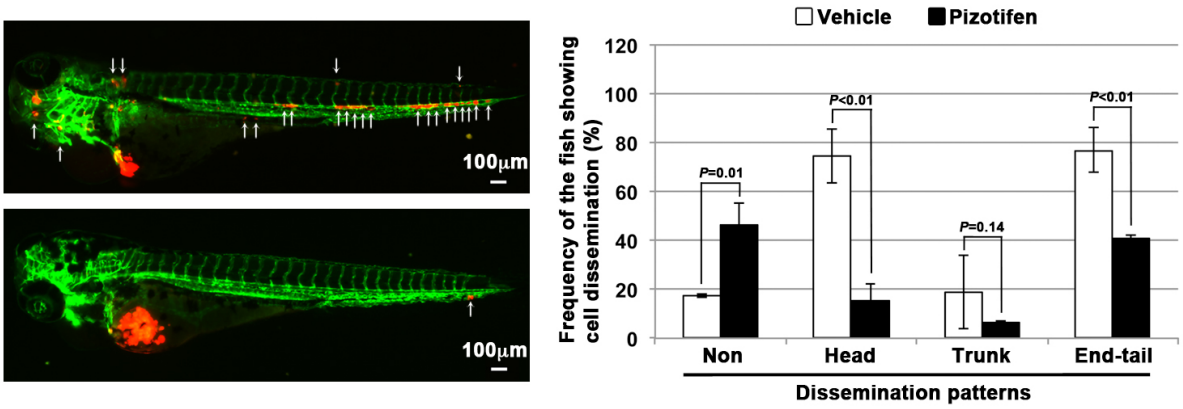

691

692 **Figure S3. Pizotifen suppressed metastatic dissemination of human pancreatic**

693 **cancer cells in a zebrafish xenotransplantation model.**

694 Related to Figure 2.

695 Representative images of dissemination of MIA-PaCa2 cells in zebrafish

696 xenotransplantation model. The fish were inoculated with MIA-PaCa2 cells, and treated

697 with either vehicle (top left) or drug (lower left). White arrows heads indicate

698 disseminated MIA-PaCa2 cells. The images were shown in 4x magnification. Scale bar,

699 100μm. The mean frequencies of the fish showing head, trunk, or end-tail dissemination

700 were tabulated (right). Each value is indicated as the mean ± SEM of two independent

701 experiments. Statistical analysis was determined by Student's *t* test.

702

703 **Table S1. A list of the genes that are involved between gastrulation and**
704 **metastasis progression**
705

Genes	Gastrulation Defects	Ref	Effects in Metastasis	Ref
BMP	Convergence and extension	(1)	EMT	(2)
WNT	Convergence and extension	(3)	Migration and Invasion	(4)
FGF	Convergence and extension	(5)	Invision	(6)
EGF	Epiboly	(7)	Migration	(8)
PDGF	Convergence and extension	(9)	EMT	(10)
CXCL12	Migration of endodermal cells	(11)	Migration and Invasion	(12)
CXCR4	Migration of endodermal cells	(11)	Migration and Invasion	(12)
PIK3CA	Convergence and extension	(13)	Migration and Invasion	(14)
YES	Epiboly	(15)	Migration	(16)
FYN	Epiboly	(17)	Migration and Invasion	(18)
MAPK1	Epiboly	(19)	Migration	(20)
SHP2	Convergence and extension	(21)	Migration	(22)
SNAI1	Convergence and extension	(23)	EMT	(24)
SNAI2	Mesoderm & Neural crest formation	(25)	EMT	
TWIST1	Mesoderm formation	(26)	EMT	(27)
TBXT	Convergence and extension	(3)	EMT	(28)
ZEB1	Epiboly	(29)	EMT	(30)
GSC	Mesodermal patterning	(31)	EMT	(32)
FOXC2	Unclear, defects in gastrulation	(33)	EMT	(34)
STAT3	Convergence and extension	(35)	Migration	(36)
POU5F1	Epiboly	(37)	EMT	(38)
EZH2	Unclear, defects in gastrulation	(39)	Invasion	(40)
EHMT2	Defects in Neurogenesis	(41)	Migration and Invasion	(42)
BMI1	Defects in skelton formation	(43)	EMT	(44)
RHOA	Convergence and extension	(45)	Migration and Invasion	(46)
CDC42	Convergence and extension	(47)	Migration and Invasion	(48)
RAC1	Convergence and extension	(49)	Migration and Invasion	(50)
ROCK2	Convergence and extension	(51)	Migration and Invasion	(52)
PAR1	Convergence and extension	(53)	Migration	(54)
PRKCI	Convergence and extension	(53)	EMT	(55)
CAP1	Convergence and extension	(56)	Migration	(57)
EZR	Epiboly	(58)	Migration	(59)
EPCAM	Epiboly	(60)	Migration and Invasion	(61)
ITGB1 / ITA5	Mesodermal Migration	(62)	Migration and Invasion	(63)
FN1	Convergence and extension	(64)	Invasion	(65)
HAS2	Dorsal migration of lateral cells	(66)	Invasion	(67)
MMP14	Convergence and extension	(68)	Invasion	(69)
COX1	Epiboly	(70)	Invasion	(71)
PTGES	Convergence and extension	(72)	Invasion	(73)
SLC39A6	Aterior migration	(74)	EMT	(75)
GNA12 / 13	Convergence and extension	(41)	Migration and Invasion	(76)
OGT	Epiboly	(77)	Migration and Invasion	(78)
CCN1	Cell Movement	(79)	Migration and Invasion	(80)
TRPM7	Convergence and extension	(81)	Migration	(82)
MAPKAPK2	Epiboly	(83)	Migration	(84)
B4GALT1	Convergence and extension	(85)	Invasion	(86)
IER2	Convergence and extension	(87)	Migration	(88)
TIP1	Convergence and extension	(89)	Migration and Invasion	(90)
PAK5	Convergence and extension	(91)	Migration	(92)
MARCKS	Convergence and extension	(93)	Migration and Invasion	(94)

706

707 **Table S1.**

708 A list of the fifty genes that play essential role in governing both metastasis and

709 gastrulation progression. The gastrulation defects in Xenopus or zebrafish that are

710 induced by knockdown of each of these genes, were indicated. The molecular

711 mechanism in metastasis that are inhibited by knockdown of each of the same genes,

712 were indicated.

713 **Table S2. A list of the drugs that interfere with epiboly progression in zebrafish**
714

Chemical name	Chemical formula	Effect of 10uM	Effect of 50uM
Acitretin	C21H26O3	Delayed	Delayed
Adrenosterone	C19H24O3	Delayed	Delayed
Albendazole	C12H15N3O2S	Severe delayed	Severe delayed
Alfadolone acetate	C23H34O5	Delayed	Delayed
Alfaxalone	C21H32O3	Delayed	Delayed
Alprostadil	C20H34O5	Delayed	Delayed
Altrenogest	C21H26O2	Slightly delayed	Delayed
Ampiroxicam	C20H21N3O7S	Non effect	Delayed
Anethole-trithione	C10H8OS3	Delayed	Delayed
Antimycin A	C28H40N2O9	Delayed	Delayed
Avobenzone	C20H22O3	Delayed	Delayed
Benzoxiquine	C16H11NO2	Non effect	Delayed
Bosentan	C27H29N5O6S	Delayed	Delayed
Butoconazole nitrate	C19H18Cl3N3O3S	Delayed	Toxic lethal
Camptothecine (S,+)	C20H16N2O4	Severe delayed	Severe delayed
Carbenoxolone disodium salt	C34H48Na2O7	Delayed	Toxic lethal
Carmofur	C11H16FN3O3	Slightly delayed	Delayed
Carprofen	C15H12ClNO2	Severe delayed	Toxic lethal
Cefdinir	C14H13N5O5S2	Delayed	Delayed
Celecoxib	C17H14F3N3O2S	Delayed	Delayed
Chlorambucil	C14H19Cl2NO2	Slightly delayed	Delayed
Chlorhexidine	C22H30Cl2N10	Non effect	Toxic lethal
Ciclopirox ethanolamine	C14H24N2O3	Delayed	Severe delayed
Cinoxacin	C12H10N2O5	Delayed	Severe delayed
Clofibrate	C12H15ClO3	Non effect	Severe delayed
Clopidogrel	C16H16ClNO2S	Non effect	Delayed
Clorgyline hydrochloride	C13H16Cl3NO	Delayed	Delayed
Colchicine	C22H25NO6	Non effect	Delayed
Deptropine citrate	C29H35NO8	Delayed	Delayed
Desipramine hydrochloride	C18H23ClN2	Delayed	Delayed
Diclofenac sodium	C14H10Cl2NNaO2	Delayed	Severe delayed
Dicumarol	C19H12O6	Delayed	Severe delayed
Diethylstilbestrol	C18H20O2	Delayed	Toxic lethal
Dimaprit dihydrochloride	C6H17Cl2N3S	Slightly delayed	Delayed
Disulfiram	C10H20N2S4	Delayed	Delayed
Dopamine hydrochloride	C8H12ClNO2	Delayed	Delayed
Eburnamonine (-)	C19H22N2O	Delayed	Delayed
Ethaverine hydrochloride	C24H30ClNO4	Delayed	Delayed
Ethinylestradiol	C20H24O2	Delayed	Severe delayed
Ethopropazine hydrochloride	C19H25ClN2S	Delayed	Delayed
Ethoxyquin	C14H19NO	Non effect	Delayed
Exemestane	C20H24O2	Slightly delayed	Delayed
Ezetimibe	C24H21F2NO3	Slightly delayed	Delayed
Fenbendazole	C15H13N3O2S	Non effect	Delayed
Fenoprofen calcium salt dihydrate	C30H30CaO8	Slightly delayed	Delayed
Fentiazac	C17H12ClNO2S	Toxic lethal	Toxic lethal
Floxuridine	C9H11FN2O5	Delayed	Toxic lethal
Flunixin meglumine	C21H28F3N3O7	Delayed	Toxic lethal
Flutamide	C11H11F3N2O3	Delayed	Toxic lethal
Fluticasone propionate	C25H31F3O5S	Non effect	Delayed
Furosemide	C12H11ClN2O5S	Delayed	Delayed
Gatifloxacin	C19H22FN3O4	Delayed	Delayed
Gemcitabine	C9H11F2N3O4	Delayed	Delayed
Gemfibrozil	C15H22O3	Delayed	Toxic lethal
Gestrinone	C21H24O2	Delayed	Delayed
Haloprogin	C9H4Cl3IO	Delayed	Toxic lethal
Hexachlorophene	C13H6Cl6O2	Delayed	Severe delayed
Hexestrol	C18H22O2	Slightly delayed	Delayed
Ibudilast	C14H18N2O	Non effect	Delayed
Idazoxan hydrochloride	C11H13ClN2O2	Slightly delayed	Delayed
Idazoxan hydrochloride	C11H13ClN2O2	Non effect	Delayed

Idebenone	C19H30O5	Severe delayed	Toxic lethal
Indomethacin	C19H16ClNO4	Non effect	Delayed
Ipriflavone	C18H16O3	Delayed	Severe delayed
Isotretinoin	C20H28O2	Non effect	Severe delayed
Isradipine	C19H21N3O5	Non effect	Delayed
Lansoprazole	C16H14F3N3O2S	Slightly delayed	Delayed
Latanoprost	C26H40O5	Non effect	Delayed
Leflunomide	C12H9F3N2O2	Delayed	Severe delayed
Letrozole	C17H11N5	Non effect	Delayed
Lithocholic acid	C24H40O3	Non effect	Delayed
Lodoxamide	C11H6ClN3O6	Non effect	Delayed
Lofepramine	C26H27ClN2O	Non effect	Delayed
Loratadine	C22H23ClN2O2	Delayed	Delayed
Loxapine succinate	C22H24ClN3O5	Delayed	Delayed
Mebendazole	C16H13N3O3	Severe delayed	Severe delayed
Mebendazole	C22H26N2O2	Non effect	Delayed
Meloxicam	C14H13N3O4S2	Delayed	Toxic lethal
Methiazole	C12H15N3O2S	Delayed	Delayed
Mevastatin	C23H34O5	Non effect	Delayed
MK 801 hydrogen maleate	C20H19NO4	Slightly delayed	Delayed
Nabumetone	C15H16O2	Non effect	Severe delayed
Naftopidil dihydrochloride	C24H30Cl2N2O3	Slightly delayed	Delayed
Nandrolone	C18H26O2	Delayed	Delayed
Naproxen sodium salt	C14H13NaO3	Delayed	Delayed
Niclosamide	C13H8Cl2N2O4	Delayed	Delayed
Nifekalant	C19H27N5O5	Delayed	Delayed
Niflumic acid	C13H9F3N2O2	Delayed	Delayed
Nimesulide	C13H12N2O5S	Non effect	Delayed
Nisoldipine	C20H24N2O6	Delayed	Toxic lethal
Nitazoxanide	C12H9N3O5S	Severe delayed	Severe delayed
Norethindrone	C20H26O2	Non effect	Delayed
Norgestimate	C23H31NO3	Slightly delayed	Delayed
Oxfendazol	C15H13N3O3S	Slightly delayed	Delayed
Oxibendazol	C12H15N3O3	Severe delayed	Severe delayed
Oxymetholone	C21H32O3	Slightly delayed	Delayed
Parbendazole	C13H17N3O2	Severe delayed	Severe delayed
Parthenolide	C15H20O3	Non effect	Delayed
Penciclovir	C10H15N5O3	Non effect	Delayed
Pentobarbital	C11H18N2O3	Non effect	Delayed
Phenazopyridine hydrochloride	C11H12ClN5	Delayed	Toxic lethal
Phenothiazine	C12H9NS	Non effect	Delayed
Phenoxybenzamine hydrochloride	C18H23Cl2NO	Non effect	Delayed
Pizotifen malate	C23H27NO5S	Delayed	Severe delayed
Pramoxine hydrochloride	C17H28ClNO3	Slightly delayed	Delayed
Prilocaine hydrochloride	C13H21ClN2O	Non effect	Delayed
Primidone	C12H14N2O2	Slightly delayed	Delayed
Racecadotril	C21H23NO4S	Slightly delayed	Delayed
Riluzole hydrochloride	C8H6ClF3N2OS	Non effect	Delayed
Ritonavir	C37H48N6O5S2	Non effect	Severe delayed
S(-)Eticlopride hydrochloride	C17H26Cl2N2O3	Delayed	Delayed
Salmeterol	C25H37NO4	Non effect	Delayed
Streptomycin sulfate	C42H84N14O36S3	Non effect	Delayed
Sulconazole nitrate	C18H16Cl3N3O3S	Delayed	Delayed
Tegafur	C8H9FN2O3	Delayed	Delayed
Telmisartan	C33H30N4O2	Severe delayed	Toxic lethal
Tenatoprazole	C16H18N4O3S	Non effect	Delayed
Terbinafine	C21H25N	Non effect	Delayed
Thimerosal	C9H9HgNaO2S	Non effect	Delayed
Thiorphan	C12H15NO3S	Delayed	Delayed
Tolcapone	C14H11NO5	Severe delayed	Severe delayed
Topotecan	C23H23N3O5	Delayed	Delayed
Tracazolate hydrochloride	C16H25ClN4O2	Severe delayed	Delayed
Tribenoside	C29H34O6	Delayed	Delayed
Triclabendazole	C14H9Cl3N2OS	Delayed	Delayed
Triclosan	C12H7Cl3O2	Delayed	Severe delayed

Trioxsalen	C14H12O3	Delayed	Delayed
Troglitazone	C24H27NO5S	Severe delayed	Toxic lethal
Valproic acid	C8H16O2	Non effect	Delayed
Voriconazole	C16H14F3N5O	Non effect	Delayed
Zardaverine	C12H10F2N2O3	Slightly delayed	Delayed
Zuclopenthixol dihydrochloride	C22H27Cl3N2OS	Delayed	Delayed

Table S2. A list of the drugs that interfere with epiboly progression in zebrafish.

Related to Figure 1.

A list of positive "hit" drugs that interfered with epiboly progression. Gastrulation defects or status of each of the zebrafish embryos that were treated with either 10μM or 50μM concentrations, are indicated.

References for Table S1.

1. Kondo M (2007) Bone morphogenetic proteins in the early development of zebrafish. *FEBS J* 274(12):2960-2967.
2. Katsuno Y, *et al.* (2008) Bone morphogenetic protein signaling enhances invasion and bone metastasis of breast cancer cells through Smad pathway. *Oncogene* 27(49):6322-6333.
3. Tada M & Smith JC (2000) Xwnt11 is a target of Xenopus Brachyury: regulation of gastrulation movements via Dishevelled, but not through the canonical Wnt pathway. *Development* 127:2227-2238.
4. Vincan E & Barker N (2008) The upstream components of the Wnt signalling pathway in the dynamic EMT and MET associated with colorectal cancer progression. *Clin Exp Metastasis* 25(6):657-663.
5. Yang X, Dormann D, Munsterberg AE, & Weijer CJ (2002) Cell movement patterns during gastrulation in the chick are controlled by positive and negative chemotaxis mediated by FGF4 and FGF8. *Dev Cell* 3(3):425-437.
6. Nomura S, *et al.* (2008) FGF10/FGFR2 signal induces cell migration and invasion in pancreatic cancer. *Br J Cancer* 99(2):305-313.
7. Song S, *et al.* (2013) Pou5f1-dependent EGF expression controls E-cadherin endocytosis, cell adhesion, and zebrafish epiboly movements. *Dev Cell* 24(5):486-501.
8. Lu Z, Jiang G, Blume-Jensen P, & Hunter T (2001) Epidermal growth factor-induced tumor cell invasion and metastasis initiated by dephosphorylation and downregulation of focal adhesion kinase. *Mol Cell Biol* 21(12):4016-4031.
9. Damm EW & Winklbauer R (2011) PDGF-A controls mesoderm cell orientation and radial intercalation during Xenopus gastrulation. *Development* 138(3):565-575.
10. Jechlinger M, *et al.* (2006) Autocrine PDGFR signaling promotes mammary cancer metastasis. *J Clin Invest* 116(6):1561-1570.
11. Mizoguchi T, Verkade H, Heath JK, Kuroiwa A, & Kikuchi Y (2008) Sdf1/Cxcr4 signaling controls the dorsal migration of endodermal cells during zebrafish gastrulation. *Development* 135(15):2521-2529.

754 12. Shen HB, Gu ZQ, Jian K, & Qi J (2013) CXCR4-mediated Stat3 activation is
755 essential for CXCL12-induced cell invasion in bladder cancer. *Tumour Biol*
756 34(3):1839-1845.
757 13. Montero J-A, Kilian B, Chan J, Bayliss PE, & Heisenberg C-P (2003)
758 Phosphoinositide 3-Kinase Is Required for Process Outgrowth and Cell
759 Polarization of Gastrulating Mesendodermal Cells. *Current Biology*
760 13(15):1279-1289.
761 14. Wander SA*, et al.* (2013) PI3K/mTOR inhibition can impair tumor
762 invasion and metastasis in vivo despite a lack of antiproliferative action in
763 vitro: implications for targeted therapy. *Breast Cancer Res Treat*
764 138(2):369-381.
765 15. Tsai WB, Zhang X, Sharma D, Wu W, & Kinsey WH (2005) Role of Yes
766 kinase during early zebrafish development. *Dev Biol* 277(1):129-141.
767 16. Barraclough J, Hodgkinson C, Hogg A, Dive C, & Welman A (2007)
768 Increases in c-Yes Expression Level and Activity Promote Motility But Not
769 Proliferation of Human Colorectal Carcinoma Cells. *Neoplasia* 9(9):745-
770 IN732.
771 17. Sharma D, Holets L, Zhang X, & Kinsey WH (2005) Role of Fyn kinase in
772 signaling associated with epiboly during zebrafish development. *Dev Biol*
773 285(2):462-476.
774 18. Yadav V & Denning MF (2011) Fyn is induced by Ras/PI3K/Akt signaling
775 and is required for enhanced invasion/migration. *Mol Carcinog* 50(5):346-
776 352.
777 19. Krens SF*, et al.* (2008) Distinct functions for ERK1 and ERK2 in cell
778 migration processes during zebrafish gastrulation. *Dev Biol* 319(2):370-
779 383.
780 20. Radtke S, Milanovic M, & Rossé C (2013) ERK2 but not ERK1 mediates
781 HGF-induced motility in non-small cell lung carcinoma cell lines. *J Cell Sci.*
782 126(Pt11):2381-2391.
783 21. Jopling C, van Geemen D, & den Hertog J (2007) Shp2 knockdown and
784 Noonan/LEOPARD mutant Shp2-induced gastrulation defects. *PLoS Genet*
785 3(12):e225.
786 22. Wang FM*, et al.* (2005) SHP-2 promoting migration and metastasis of
787 MCF-7 with loss of E-cadherin, dephosphorylation of FAK and secretion of
788 MMP-9 induced by IL-1beta in vivo and in vitro. *Breast Cancer Res Treat*
789 89(1):5-14.
790 23. Ip YT & Gridley T (2002) Cell movements during gastrulation: snail
791 dependent and independent pathways. *Curr Opin Genet Dev* 12(4):423-
792 429.
793 24. Batlle E, Sancho E, Francí C, Domínguez D, & Monfar M (2000) The
794 transcription factor snail is a repressor of E-cadherin gene expression in
795 epithelial tumour cells. *Nat Cell Biol* 2(2):84-89.
796 25. Shi J, Severson C, Yang J, Wedlich D, & Klymkowsky MW (2011) Snail2
797 controls mesodermal BMP/Wnt induction of neural crest. *Development*
798 138(15):3135-3145.
799 26. Castanon I & Baylies MK (2002) A Twist in fate: evolutionary comparison
800 of Twist structure and function. *Gene* 287(1-2):11-22.
801 27. Yang J*, et al.* (2004) Twist, a master regulator of morphogenesis, plays an
802 essential role in tumor metastasis. *Cell* 117(7):927-939.

803 28. Fernando RI, *et al.* (2010) The T-box transcription factor Brachyury
804 promotes epithelial-mesenchymal transition in human tumor cells. *J Clin*
805 *Invest* 120(2):533-544.
806 29. Vannier C, Mock K, Brabletz T, & Driever W (2013) Zeb1 regulates E-
807 cadherin and Epcam (epithelial cell adhesion molecule) expression to
808 control cell behavior in early zebrafish development. *J Biol Chem*
809 288(26):18643-18659.
810 30. Spaderna S, *et al.* (2008) The transcriptional repressor ZEB1 promotes
811 metastasis and loss of cell polarity in cancer. *Cancer Res* 68(2):537-544.
812 31. Sander V, Reversade B, & De Robertis EM (2007) The opposing homeobox
813 genes Goosecoid and Vent1/2 self-regulate Xenopus patterning. *EMBO J*
814 26(12):2955-2965.
815 32. Hartwell KA, *et al.* (2006) The Spemann organizer gene, Goosecoid,
816 promotes tumor metastasis. *Proc Natl Acad Sci U S A* 103(50):18969-
817 18974.
818 33. Wilm B, James RG, Schultheiss TM, & Hogan BL (2004) The forkhead
819 genes, Foxc1 and Foxc2, regulate paraxial versus intermediate mesoderm
820 cell fate. *Dev Biol* 271(1):176-189.
821 34. Mani SA, *et al.* (2007) Mesenchyme Forkhead 1 (FOXC2) plays a key role
822 in metastasis and is associated with aggressive basal-like breast cancers.
823 *Proc Natl Acad Sci U S A* 104(24):10069-10074.
824 35. Miyagi C, *et al.* (2004) STAT3 noncell-autonomously controls planar cell
825 polarity during zebrafish convergence and extension. *J Cell Biol*
826 166(7):975-981.
827 36. Abdulghani J, *et al.* (2008) Stat3 promotes metastatic progression of
828 prostate cancer. *Am J Pathol* 172(6):1717-1728.
829 37. Lachnit M, Kur E, & Driever W (2008) Alterations of the cytoskeleton in all
830 three embryonic lineages contribute to the epiboly defect of Pou5f1/Oct4
831 deficient MZspg zebrafish embryos. *Dev Biol* 315(1):1-17.
832 38. Dai X, *et al.* (2013) OCT4 regulates epithelial-mesenchymal transition and
833 its knockdown inhibits colorectal cancer cell migration and invasion.
834 *Oncol Rep* 29(1):155-160.
835 39. O'Carroll D, *et al.* (2001) The polycomb-group gene Ezh2 is required for
836 early mouse development. *Mol Cell Biol* 21(13):4330-4336.
837 40. Ren G, *et al.* (2012) Polycomb protein EZH2 regulates tumor invasion via
838 the transcriptional repression of the metastasis suppressor RKIP in breast
839 and prostate cancer. *Cancer Res* 72(12):3091-3104.
840 41. Lin F, *et al.* (2005) Essential roles of G{alpha}12/13 signaling in distinct
841 cell behaviors driving zebrafish convergence and extension gastrulation
842 movements. *J Cell Biol* 169(5):777-787.
843 42. Chen MW, *et al.* (2010) H3K9 histone methyltransferase G9a promotes
844 lung cancer invasion and metastasis by silencing the cell adhesion
845 molecule Ep-CAM. *Cancer Res* 70(20):7830-7840.
846 43. van der Lugt NM, *et al.* (1994) Posterior transformation, neurological
847 abnormalities, and severe hematopoietic defects in mice with a targeted
848 deletion of the bmi-1 proto-oncogene. *Genes Dev* 8(7):757-769.
849 44. Guo BH, *et al.* (2011) Bmi-1 promotes invasion and metastasis, and its
850 elevated expression is correlated with an advanced stage of breast cancer.
851 *Mol Cancer* 10(1):10.
852 45. Zhu S, Liu L, Korzh V, Gong Z, & Low BC (2006) RhoA acts downstream of
853 Wnt5 and Wnt11 to regulate convergence and extension movements by

854 involving effectors Rho kinase and Diaphanous: use of zebrafish as an in
855 vivo model for GTPase signaling. *Cell Signal* 18(3):359-372.
856 46. Yoshioka K, Nakamori S, & Itoh K (1999) Overexpression of small GTP-
857 binding protein RhoA promotes invasion of tumor cells. *Cancer Res*
858 59(8):2004-2010.
859 47. Choi SC & Han JK (2002) Xenopus Cdc42 regulates convergent extension
860 movements during gastrulation through Wnt/Ca2+ signaling pathway.
861 *Dev Biol* 244(2):342-357.
862 48. Reymond N, *et al.* (2012) Cdc42 promotes transendothelial migration of
863 cancer cells through beta1 integrin. *J Cell Biol* 199(4):653-668.
864 49. Habas R, Dawid IB, & He X (2003) Coactivation of Rac and Rho by
865 Wnt/Frizzled signaling is required for vertebrate gastrulation. . *Genes Dev*
866 17(2):295-309.
867 50. Vega FM & Ridley AJ (2008) Rho GTPases in cancer cell biology. *FEBS Lett*
868 582(14):2093-2101.
869 51. Marlow F, Topczewski J, Sepich D, & Solnica-Krezel L (2002) Zebrafish
870 Rho kinase 2 acts downstream of Wnt11 to mediate cell polarity and
871 effective convergence and extension movements. *Curr Biol* 12(11):876-
872 884.
873 52. Itoh K, *et al.* (1999) An essential part for Rho-associated kinase in the
874 transcellular invasion of tumor cells. *Nat Med* 5(2):221-225.
875 53. Kusakabe M & Nishida E (2004) The polarity-inducing kinase Par-1
876 controls Xenopus gastrulation in cooperation with 14-3-3 and aPKC.
877 *EMBO J* 23(21):4190-4201.
878 54. Shi X, Gangadharan B, Brass LF, Ruf W, & Mueller BM (2004) Protease-
879 activated receptors (PAR1 and PAR2) contribute to tumor cell motility
880 and metastasis. *Mol Cancer Res* 2(7):395-402.
881 55. Gunaratne A, Thai BL, & Di Guglielmo GM (2013) Atypical protein kinase C
882 phosphorylates Par6 and facilitates transforming growth factor beta-
883 induced epithelial-to-mesenchymal transition. *Mol Cell Biol* 33(5):874-
884 886.
885 56. Seifert K, Ibrahim H, Stodtmeister T, Winklbauer R, & Niessen CM (2009)
886 An adhesion-independent, aPKC-dependent function for cadherins in
887 morphogenetic movements. *J Cell Sci* 122(Pt 14):2514-2523.
888 57. Yamazaki K, *et al.* (2009) Adenylate cyclase-associated protein 1
889 overexpressed in pancreatic cancers is involved in cancer cell motility.
890 *Lab Invest* 89(4):425-432.
891 58. Link V, *et al.* (2006) Identification of regulators of germ layer
892 morphogenesis using proteomics in zebrafish. *J Cell Sci* 119(Pt 10):2073-
893 2083.
894 59. Khanna C, *et al.* (2004) The membrane-cytoskeleton linker ezrin is
895 necessary for osteosarcoma metastasis. *Nat Med* 10(2):182-186.
896 60. Slanchev K, *et al.* (2009) The epithelial cell adhesion molecule EpCAM is
897 required for epithelial morphogenesis and integrity during zebrafish
898 epiboly and skin development. *PLoS Genet* 5(7):e1000563.
899 61. Ni J, *et al.* (2012) Role of the EpCAM (CD326) in prostate cancer
900 metastasis and progression. *Cancer Metastasis Rev* 31(3-4):779-791.
901 62. Skalski M, Alfandari D, & Darribere T (1998) A key function for alphav
902 containing integrins in mesodermal cell migration during Pleurodeles
903 waltl gastrulation. *Dev Biol* 195(2):158-173.

904 63. Felding-Habermann B (2003) Integrin adhesion receptors in tumor
905 metastasis. *Clin Exp Metastasis* 20(3):203-213.
906 64. Marsden M & DeSimone DW (2003) Integrin-ECM Interactions Regulate
907 Cadherin-Dependent Cell Adhesion and Are Required for Convergent
908 Extension in Xenopus. *Current Biology* 13(14):1182-1191.
909 65. Malik G, *et al.* (2010) Plasma fibronectin promotes lung metastasis by
910 contributions to fibrin clots and tumor cell invasion. *Cancer Res*
911 70(11):4327-4334.
912 66. Bakkers J, *et al.* (2004) Has2 is required upstream of Rac1 to govern
913 dorsal migration of lateral cells during zebrafish gastrulation.
914 *Development* 131(3):525-537.
915 67. Kim HR, *et al.* (2004) Hyaluronan facilitates invasion of colon carcinoma
916 cells in vitro via interaction with CD44. *Cancer Res* 64(13):4569-4576.
917 68. Coyle RC, Latimer A, & Jessen JR (2008) Membrane-type 1 matrix
918 metalloproteinase regulates cell migration during zebrafish gastrulation:
919 evidence for an interaction with non-canonical Wnt signaling. *Exp Cell Res*
920 314(10):2150-2162.
921 69. Perentes JY, *et al.* (2011) Cancer cell-associated MT1-MMP promotes
922 blood vessel invasion and distant metastasis in triple-negative mammary
923 tumors. *Cancer Res* 71(13):4527-4538.
924 70. Cha YI, *et al.* (2006) Cyclooxygenase-1-derived PGE2 promotes cell
925 motility via the G-protein-coupled EP4 receptor during vertebrate
926 gastrulation. *Genes Dev* 20(1):77-86.
927 71. Kundu N & Fulton AM (2002) Selective cyclooxygenase (COX)-1 or COX-2
928 inhibitors control metastatic disease in a murine model of breast cancer.
929 *Cancer Res* 62(8):2343-2346.
930 72. Speirs CK, *et al.* (2010) Prostaglandin Gbetagamma signaling stimulates
931 gastrulation movements by limiting cell adhesion through Snai1a
932 stabilization. *Development* 137(8):1327-1337.
933 73. Wang D & Dubois RN (2006) Prostaglandins and cancer. *Gut* 55(1):115-
934 122.
935 74. Yamashita S, *et al.* (2004) Zinc transporter LIVI controls epithelial-
936 mesenchymal transition in zebrafish gastrula organizer. *Nature*
937 429(6989):298-302.
938 75. Lue HW, *et al.* (2011) LIV-1 promotes prostate cancer epithelial-to-
939 mesenchymal transition and metastasis through HB-EGF shedding and
940 EGFR-mediated ERK signaling. *PLoS One* 6(11):e27720.
941 76. Yagi H, *et al.* (2011) A synthetic biology approach reveals a CXCR4-G13-
942 Rho signaling axis driving transendothelial migration of metastatic breast
943 cancer cells. *Sci Signal* 4(191):ra60.
944 77. Webster DM, *et al.* (2009) O-GlcNAc modifications regulate cell survival
945 and epiboly during zebrafish development. *BMC Dev Biol* 9:28.
946 78. Lynch TP, *et al.* (2012) Critical role of O-Linked beta-N-acetylglucosamine
947 transferase in prostate cancer invasion, angiogenesis, and metastasis. *J*
948 *Biol Chem* 287(14):11070-11081.
949 79. Latinkic BV (2003) Xenopus Cyr61 regulates gastrulation movements and
950 modulates Wnt signalling. *Development* 130(11):2429-2441.
951 80. Lin J, *et al.* (2012) A novel anti-Cyr61 antibody inhibits breast cancer
952 growth and metastasis in vivo. *Cancer Immunol Immunother* 61(5):677-
953 687.

954 81. Liu W, *et al.* (2011) TRPM7 regulates gastrulation during vertebrate
955 embryogenesis. *Dev Biol* 350(2):348-357.
956 82. Middelbeek J, *et al.* (2012) TRPM7 is required for breast tumor cell
957 metastasis. *Cancer Res* 72(16):4250-4261.
958 83. Holloway BA, *et al.* (2009) A novel role for MAPKAPK2 in morphogenesis
959 during zebrafish development. *PLoS Genet* 5(3):e1000413.
960 84. Kumar B, *et al.* (2010) p38 mitogen-activated protein kinase-driven
961 MAPKAPK2 regulates invasion of bladder cancer by modulation of MMP-2
962 and MMP-9 activity. *Cancer Res* 70(2):832-841.
963 85. Machingo QJ, Fritz A, & Shur BD (2006) A beta1,4-galactosyltransferase is
964 required for convergent extension movements in zebrafish. *Dev Biol*
965 297(2):471-482.
966 86. Zhu X, *et al.* (2005) Elevated beta1,4-galactosyltransferase I in highly
967 metastatic human lung cancer cells. Identification of E1AF as important
968 transcription activator. *J Biol Chem* 280(13):12503-12516.
969 87. Hong SK, Tanegashima K, & Dawid IB (2011) XIer2 is required for
970 convergent extension movements during Xenopus development. *Int J Dev*
971 *Biol* 55(10-12):917-921.
972 88. Neeb A, *et al.* (2012) The immediate early gene Ier2 promotes tumor cell
973 motility and metastasis, and predicts poor survival of colorectal cancer
974 patients. *Oncogene* 31(33):3796-3806.
975 89. Besser J, Leito JT, van der Meer DL, & Bagowski CP (2007) Tip-1 induces
976 filopodia growth and is important for gastrulation movements during
977 zebrafish development. *Dev Growth Differ* 49(3):205-214.
978 90. Han M, Wang H, Zhang HT, & Han Z (2012) The PDZ protein TIP-1
979 facilitates cell migration and pulmonary metastasis of human invasive
980 breast cancer cells in athymic mice. *Biochem Biophys Res Commun*
981 422(1):139-145.
982 91. Faure S, *et al.* (2005) Xenopus p21-activated kinase 5 regulates
983 blastomeres' adhesive properties during convergent extension
984 movements. *Dev Biol* 277(2):472-492.
985 92. Gong W, *et al.* (2009) P21-activated kinase 5 is overexpressed during
986 colorectal cancer progression and regulates colorectal carcinoma cell
987 adhesion and migration. *Int J Cancer* 125(3):548-555.
988 93. Iioka H, Ueno N, & Kinoshita N (2004) Essential role of MARCKS in cortical
989 actin dynamics during gastrulation movements. *J Cell Biol* 164(2):169-
990 174.
991 94. Rombouts K, *et al.* (2013) Myristoylated Alanine-Rich protein Kinase C
992 Substrate (MARCKS) expression modulates the metastatic phenotype in
993 human and murine colon carcinoma in vitro and in vivo. *Cancer Lett*
994 333(2):244-252.
995

996
997